Check for updates

RESEARCH ARTICLE

Key Points:
- Despite being geomorphically diverse, the size distributions of riverbed gravel on three alluvial fans are shown to be self-similar
- The mobility of bedload is quantified using a self-similar relative mobility transfer function for size-selective transport
- Only the coarsest tails of the bed surface size distributions appear sensitive to the rivers' geomorphic evolution

Evidence for Self-Similar Bedload Transport on Andean Alluvial Fans, Iglesia Basin, South Central Argentina

R. M. Harries[1] iD, L. A. Kirstein[1] iD, A. C. Whittaker[2], M. Attal[1] iD, S. Peralta[3] iD, and S. Brooke[2] iD

[1]School of Geosciences, University of Edinburgh, Edinburgh, UK, [2]Department of Earth Science and Engineering, Imperial College London, London, UK, [3]Instituto de Geología, Universidad Nacional de San Juan, San Juan, Argentina

Abstract Self-similar downstream grain-size fining trends in fluvial deposits are being increasingly used to simplify equilibrium sediment transport dynamics in numerical models. Their ability to collapse time-averaged behavior of a depositional system into a simple mass balance framework makes them ideal for exploring the sensitivity of sediment routing systems to their climatic and tectonic boundary conditions. This is important if we want to better understand the sensitivity of landscapes to environmental change over timescales $>10^2$ years. However, the extent to which self-similarity is detectable in the deposits of natural rivers is not fully constrained. In transport-limited rivers, stored sediment can be remobilized or "recycled" and this behavior has been highlighted as a mechanism by which externally forced grain-size fining trends are distorted. Here we evaluate evidence of self-similarity in surface gravel-size distributions on three geomorphically diverse alluvial fans in the Iglesia basin, south Central Argentine Andes. We find that size distributions are self-similar, deviating from that condition only when significant variability occurs in the coarse tails of the distributions. Our analysis indicates a strong correlation between the degree of sediment recycling and the proportion of coarse clasts present on the bed surface. However, by fitting a relative mobility transfer function, we demonstrate that size-selectivity alone can explain the bulk size distributions observed. This strengthens the application of self-similar grain size fining models to solving problems of mass balance in a range of geomorphic settings, with an aim for reconstructing environmental boundary conditions from stratigraphy.

Plain Language Summary To date, little research has been conducted into how sensitively rivers respond to changes in their sediment and water supplies. This is because river processes that control how and when sediment moves are complex and evolve in response to landscape change over a wide range of time and spatial scales. Using a unique field site in the Argentine Andes, we find evidence for an important river behavior that can simplify the complexity of physical river processes in space and time. Each of three rivers investigated had sorted the gravel they transport by size, both locally on the river bed and along their downstream length. We found that at any site along the river, the degree to which the gravel is sorted is the same. This means that taking into account the change in sediment size downstream, the underlying grain size distributions are all the same. As size sorting is related to the efficiency of the river to transport its sediment load, we can use this finding to reconstruct the mobility of sediment anywhere along the river. We do this by fitting a simple and elegant transfer function to our data, which can be incorporated into models of long-term river evolution.

1. Introduction

1.1. Rationale

Understanding the sensitivity of sedimentary archives to environmental change is a key challenge in the geosciences, as it is these physical records that underpin our understanding of how tectonics, climate, and erosion have shaped the surface of our planet (e.g., Burke et al., 1990; Goodbred, 2003; Molnar & England, 1990). Alluvial fans store sediment derived directly from mountainous source regions, so their stratigraphy is, in principle, well placed to record the tectonic and climatic evolution of mountain ranges (Densmore et al., 2007; Legarreta et al., 1993). Numerical modeling and laboratory experiments demonstrate that the three dimensional architecture of an alluvial fan is linked to the spatial distribution of accommodation space in a subsiding basin, the volume, and caliber of sediment supplied to the fan apex and river discharge (Guerit et al., 2014; Hooke & Rohrer, 1979). As such, geomorphic evidence of fan aggradation, progradation, or retrogradation and surface incision are often temporally correlated with proxy records of environmental variables,

such as rates of tectonic uplift or basin subsidence and time-average precipitation or climate storminess (D'Arcy et al., 2017; Densmore et al., 2007; Savi et al., 2016).

In flume experiments, where the impact of abrasion on clast size is minimal, the total downstream length of an aggrading alluvial river is typically inherited from the rate at which river gravels fine downstream and is a function of size-selective sorting during bedload transport and deposition (Paola, Parker, et al., 1992). This systematic pattern of downstream fining is well documented for natural streamflow-dominated, alluvial gravel bed rivers (e.g., Powell, 1998; Rice, 1999), where at a channel length scale, the mean grain size of the bed surface material typically decreases exponentially downstream. Downstream fining, driven by selective deposition, is also apparent in many stratigraphic studies of fluvially dominated sediments for both Holocene and geologically older deposits (e.g., Allen et al., 2013; D'Arcy et al., 2017; Duller et al., 2010; Parsons et al., 2012). The fine-scale physics of bedload sorting is highly complex and is dependent on the evolution of sediment transport rates through time. These hydraulic details, including flow magnitudes and frequencies, are often unknowable for even the recent geologic past (Allen, 2017; Duller et al., 2010). However, work by Fedele and Paola (2007) made quantitative links between changes in the rate of downstream fining and the wider governing parameters of sediment routing systems, namely, (1) the flux and range of sediment sizes in the supply and (2) the extent and spatial distribution of deposition. Based on previous observations that rivers display self-similar bed profiles and self-similar substrate distributions (e.g., Cui et al., 1996; Hoey & Bluck, 1999; Paola, Heller, & Angevine, 1992), Fedele and Paola (2007) used similarity methods to summarize the main fluid and grain physics embodied in current sorting models, leading to simplified transport functions that could be readily included in models for the longer-term evolution of alluvial deposits and stratigraphy. In essence, they showed that the problem of downstream fining in fluvial deposits fundamentally depends on the partitioning of the total variance in the sediment supply between the variance at an individual sampling site (for instance, in a channel deposit) and the variance down the whole system, which often manifests as exponential, downstream, grain size fining (e.g., Duller et al., 2010). Self-similarity in near–steady state river long profiles (Toro-Escobar et al., 1996) and self-similarity in substrate grain size distributions (Cui et al., 1996; Paola, Heller, & Angevine, 1992; Seal et al., 1997) motivate the possibility for solving the distribution of grain sizes along a river bed, knowing only the spatial distribution of mass extraction by deposition over the long term and the time averaged, relative mobility of clast sizes.

The self-similar approach is very useful for analyzing river behavior over timescales relevant to Earth surface systems (i.e., 10^2–10^7 years). Furthermore, grain size distributions are easily measured in the field and have a good preservation potential in depositional stratigraphy. In modeling basin stratigraphy, Duller et al. (2010) demonstrate that self-similar grain size fining trends are sensitive to the wavelength of basin subsidence, the volume of sediment supplied to the apex of the depositional system, and the distribution of grain sizes in that supply. Recent inversions of grain size data collected from ancient stratigraphy and also on Pleistocene to recent fan surfaces, using the self-similarity approach, also clearly suggest a sensitivity to these variables in natural systems (Allen et al., 2017; Duller et al., 2010; Whittaker et al., 2011).

The application to natural alluvial fan stratigraphy, however, is challenged by a recognition that the processes behind stratigraphy are complex and have coupled, nonlinear relationships with climate and tectonics (Forzoni et al., 2014; Humphrey & Heller, 1995; Jerolmack & Paola, 2010). Autogenic processes that influence the geomorphic evolution of fans, including fan head entrenchment, lobe abandonment, and channel avulsions, are well documented in both experimental and natural fans across all scales (Kim et al., 2014; Nicholas & Quine, 2007; Schumm, 1979). Changes in the mass balance can lead to rivers incising and recycling sediments previously deposited, introducing sediment volumes laterally into the system (Malatesta et al., 2017; Straub & Esposito, 2013; Straub & Wang, 2013). The impact these processes have on both the proportional fractionation of grain sizes downstream and on the local substrate is unclear. Lateral inputs from tributaries, which act as point sources of sediment, have been identified as a source of noise in systematic grain size fining trends in rivers (Ferguson et al., 2006; Rice, 1999). This is evidence to suggest that lateral inputs of sediment could significantly distort patterns of grain size fining and further generate stratigraphic responses in the absence of external environmental forcing (Coulthard et al., 2005; Van De Wiel & Coulthard, 2010). The extent to which autogenic, geomorphic processes influence deposited grain size trends in natural rivers is not fully constrained.

In this paper, we explore the robustness of self-similar grain size trends on natural streamflow-dominated alluvial fans and we evaluate the extent to which these distributions can be used to gain insight into sediment dynamics, using the self-similarity approach originally introduced by Fedele and Paola (2007). Moreover, we examine the impact that sediment recycling and tributary inputs have had on the degree of self-similarity in fluvial deposits and how this might influence the sensitivity of downstream grain size fining trends to external forcing.

1.2. Self-Similarity Approach

Self-similarity among the size distributions of riverbed gravels refers to the scale invariant shape of their distribution. Downstream, the standard deviation, or variance, of surface gravels has been observed to decrease exponentially, at a rate similar to the mean, so that the degree of sorting at any point downstream is constant (Paola, Heller, & Angevine, 1992; Paola, Parker, et al., 1992; Seal et al., 1997; Toro-Escobar et al., 1996). This behavior is predictable from 1-D solutions of the Exner sediment mass balance equation using a constant value of the critical Shields parameter (i.e., the nondimensionalized critical shear stress required for particle entrainment; Paola & Voller, 2005; Shields, 1936). Here a near-bankfull threshold for sediment motion is assumed, which is appropriate for many gravel bed rivers (Andrews, 1984; Buffington, 2012; Millar, 2005; Mueller et al., 2005). Indeed, Parker et al. (2007) demonstrated that the critical Shields parameter varies only slightly with dimensionless discharge and that the ratio between the Shields parameter and the bankfull shear stress is primarily a function of bank strength. By assuming the ratio of dimensionless boundary shear stress to critical shear stress is constant, it is implied that the size distribution of clasts deposited locally emerges from a time-averaged sediment supply and flow competence and can be estimated without needing to obtain high-resolution records of variability in flow magnitude (Paola & Seal, 1995; Parker & Toro-Escobar, 2002). The timescale over which self-similarity in depositional grain size is established is unclear, though is likely intermediate, that is, long enough to smooth out the fine-scale dynamics of sediment transport, but short enough to not feel the influence of large-scale boundary conditions such as climatic, tectonic, or base-level change (Fedele & Paola, 2007). Self-similarity has previously been observed in fluvial deposits of the North Fork Toutle river (Fedele & Paola, 2007; Seal & Paola, 1995) and Holocene streamflow-dominated fan surfaces in Death Valley (D'Arcy et al., 2017). Sediment transport and deposition, typically described by Hirano's (1971) three-layer sediment sorting model, can then be expressed as a simple, probabilistic partitioning ratio between the size fraction of clasts in transport, p_i, and the size fraction on the bed surface, F_i.

$$J_i = p_i/F_i \tag{1}$$

where J_i describes the relative mobility of clast sizes deposited locally (Duller et al., 2010; Fedele & Paola, 2007). Assuming both the bed surface size distributions and the form of J can be collapsed into the same similarity solution, the bed surface size distribution can be used to reconstruct J. The existence of a self-similar solution for any grain size fraction requires that both the substrate composition F and the relative mobility function J are expressed as functions of the same similarity variable, ξ; for grain sizes coarser than sand (i.e., "gravel"), for which bed load transport is likely to be the dominant mode, the self-similar distributions of ξ are obtained from the observation that the mean and standard deviations of these sediments decay at the same rate downstream (above; see also section 3.3).

Fedele and Paola (2007) derive a function for J using a semiempirical, hydraulically based fining model, ACRONYM, calibrated against field and experimental data (Parker, 1991) and based on their transformation of the measured grain size distributions into self-similar ξ distributions. For a range of subsidence and sediment supply conditions, Fedele and Paola (2007) ran ACRONYM, holding sediment and water discharge and the input size distribution constant. Having verified scale invariance among substrate grain size distributions in the model, they then reconstructed the differential mobility and resulting fractionation of relative clast sizes, between the bedload and substrate, depending on their relative proportion in the substrate. For a full derivation see Fedele and Paola (2007), from which J is defined as

$$J_i = a_g e^{-b_g \xi} + c_g \tag{2}$$

where a_g, b_g, and c_g are constants that characterize the initial motion conditions of gravel. Sediment entrainment is considered dependent solely on dimensionless particle size; therefore, a_g scales with the mobility of all clast sizes, b_g describes the rate at which clasts of increasing size become less mobile than smaller clasts,

and c_g relates to the minimum probability of entraining a clast of any size. The shape and structure of J are expected to depend on the nature of the transport regime; the formulation above is for sediments coarser than sand (D'Arcy et al., 2017; Whittaker et al., 2011). The hydraulic geometries of gravel bed rivers are incorporated implicitly by employing threshold channel theory (Parker, 1978). Applied to field data, this relative mobility function ought, therefore, to provide useful information about the river's ability to transport its load, without the necessity for constraining variables such as channel widths, which are difficult to reconstruct back in time.

This approach predicts that the partitioning of bedload grain sizes locally conserves a constant and predictable rate of downstream grain size fining along the length of the river, normalized to account for the downstream distribution of deposition. In this paper we apply and test these ideas. We provide much-needed field data from three large and exceptionally well-exposed streamflow-dominated fans in the Iglesia basin, south Central Argentine Andes to investigate the extent to which grain size distributions record information on sediment dynamics over time, and to quantify potential sources of noise in these natural sedimentary systems. Understanding how natural variability in alluvial rivers is expressed given different allogenic and autogenic forcings is an important step toward understanding the limitations of using grain size to reconstruct environmental change. Each of the alluvial fans under investigation is large and of a scale typically preserved in the ancient stratigraphic record. These rivers are potentially challenging because they are fed by multiple sources of sediment, altering the mass balance of the sediment routing system along its length. We analyze the extent to which deposited grain size distributions in these rivers can be described by similarity in bedload transport and examine what autogenic traits are most influential in distorting downstream grain size trends.

2. Study Area

This study examines arid, catchment-alluvial fans, along the western margin of the Iglesia basin, draining the Frontal Cordillera of the south Central Argentine Andes, 30–31°S. The Iglesia basin is a narrow depression, elevated >1,000 m above sea level, on the western flank of the thrust belt and is adjacent to a region of the High Andes thought to have been tectonically stable since the Pliocene (Jordan et al., 1993). This basin is the primary depocenter and stratigraphic archive, for coarse material eroded from the High Andes.

The climate is that of an arid desert, with infrequent, high-magnitude, rainfall events. From 1960–1990, the mean annual precipitation across the range was 190 mm and the mean annual temperature was −2.2 °C (Hijmans et al., 2005). Precipitation falls predominantly as snow, where the peaks of the Frontal Cordillera are glaciated above ~4,500 m. The catchment slopes are strongly influenced by cryogenic processes (Forte et al., 2016) and are landslide dominated with localized rock slide deposits (Penna et al., 2016). The Iglesia basin itself is within the rain shadow of the range and is classified by Le Houérou et al. (2006) as hyperarid, with a mean annual precipitation of 30–60 mm and a mean annual temperature of 15.7 °C (Minetti et al., 1986). Vegetation is sparse and most of the rivers are ephemeral, only active during infrequent, intense rainfall events in the summer or during the melt season following heavy winter snowfall in the Cordillera (Perucca & Martos, 2012).

Bedrock lithologies exposed within the range are relatively resistant; they are dominated by Carboniferous to Triassic metasedimentary rocks and granitic batholiths, with outcrops of Miocene intrusive and volcanic rocks (Jones et al., 2014). Erosion rates measured across this region are low, typically ~10^{-2} mm/year (Bookhagen & Strecker, 2012; Carretier et al., 2015). Millennial erosion rates of 0.012–0.04 mm/year (Giambiagi et al., 2012; Hoke et al., 2014) and 0.06–0.1 mm/year are reported south of the Iglesia basin (32–34°S). At the same latitude, on the Chilean side of the Andes, Carretier et al. (2013) estimate <0.06 mm/year from both suspended sediment loads (10^1 years) and ^{10}Be millennial catchment average erosion rates.

The climate and the geology specific to this vast landscape, left unaltered by human activity, provide an excellent opportunity to study how unmodified alluvial fans have evolved to distribute sediment downstream and to evaluate the extent to which these fans show self-similarity in their grain-size distributions, inspired by the work of Fedele and Paola (2007). Minimal vegetation cover and negligible human influence minimizes the potential for artificial noise in grain size fining trends and allows us to isolate the influence of size selective deposition on deposited grain sizes. Furthermore, the export of lithologically hard clasts from the mountain catchments reduces the influence of abrasion on the gravel mass balance of the sediment routing system and on the rate of grain size fining over fan length scales of a few tens of kilometers.
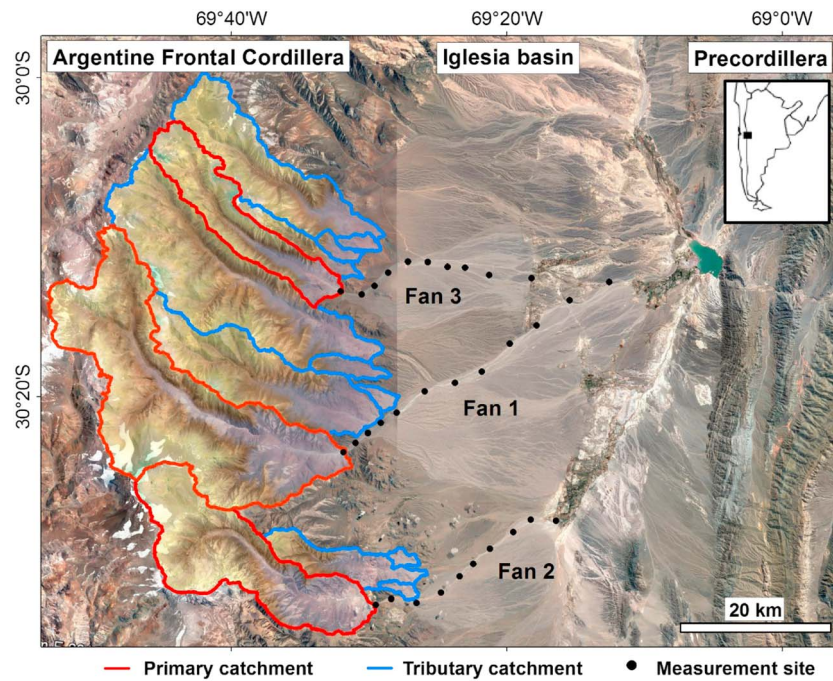
Figure 1. Location of Iglesia basin within the foreland of the Argentine Andes; bounded by the Frontal Cordillera to the west and the Precordillera to the east. On the satellite composite, the primary and tributary bedrock catchments feeding three fan systems are delineated and the circles pinpoint where the modern surface on each fan was sampled.

We have selected three large alluvial fans for study (Figure 1). Two of the catchment-fans are similar in size, ~ 25 km long in terms of depositional length, and lie north and south of a third, larger fan, ~40 km in length. Together these form a shallow sloping bajada of alluvial sediments that partially fill the basin. Each fan is fed by multiple catchments whose channels coalesce in their upper reaches. The fan heads are currently entrenched and are evacuating sediment backfilled within their catchments. The bajada is segmented by a number of terraces, elevated up to 40 m above the modern channel, at the fan head. The significant relief of two of these surfaces can be observed in Figure 2. Four generations of fan surfaces have been mapped across a central region of the bajada by Perucca and Martos (2012), who correlate the oldest surface to the Middle Pleistocene, based on a regional cross-correlation of aggradation events (Polanski, 1963), temporally constrained by cosmogenic ages on alluvial levels on El Tigre Piedmont in the Precordillera, further south (Siame et al., 1997). Perucca and Martos (2012) suggest the most recent surface, superposed <2 m above the modern channels on each fan, can be temporally correlated with Upper Pleistocene-Holocene formations in Tunuyan Mendoza (Polanski, 1963; Zarate & Mehl, 2008), ~400 km south of Iglesia. Radiocarbon dates attained for this most recent cycle of aggradation range between 1400 ± 130 ^{14}C BP and 9625 ± 200 ^{14}C BP. The modern rivers are incised along their length into this surface with a channelized braided morphology.

3. Methods

We sampled grain size on the dry river beds of three, adjacent alluvial fans and investigated the extent to which local size distributions on each fan can be modeled by self-similar size-selective deposition. We analyzed the degree of similarity between distributions on each river and apply Fedele and Paola's (2007) relative mobility transfer function to reconstruct the mobility of the gravel grain sizes deposited. The potential for grain size trends to be buffered by sediment recycling is investigated through a quantitative analysis of the sediment fluxes involved in each sediment routing system. We analyzed the significance of sediment recycling in influencing the similarity of deposited size distributions and the relative mobility of the substrate. By comparing alluvial systems, our approach allowed us to investigate the importance of autogenic, geomorphic variables in influencing deposited grains size trends.
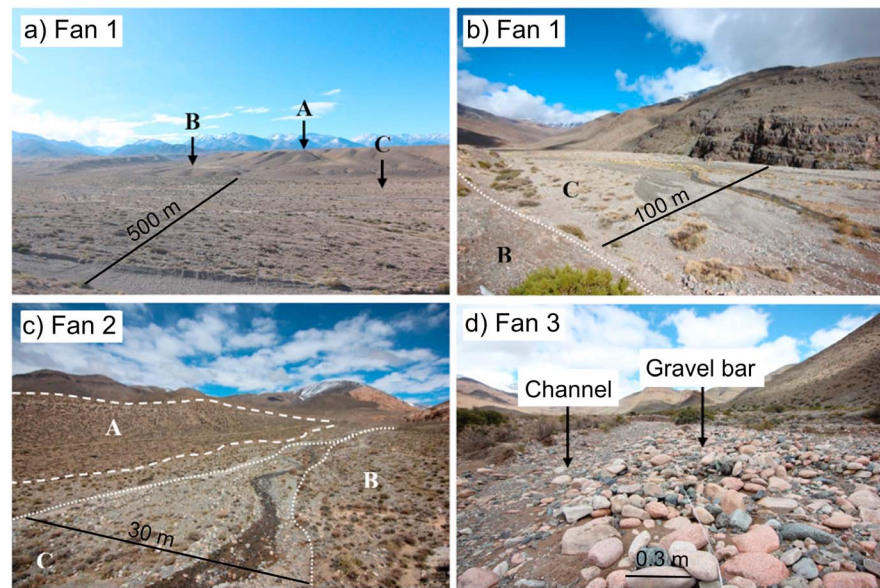
Figure 2. Photographs of Iglesia basin alluvial fans. (a) Fan 1, looking upstream toward the Andean mountain front where three alluvial surfaces can be observed. Surface C is currently being reworked by the modern channel and surfaces B and A are superelevated ~10 and 100 m above the modern channel, respectively. (b–d) Looking upstream into the catchment mouths of fans 1, 2, and 3, where surfaces A, B, and C are roughly correlated across fans based on their superposition. In photograph (d) the typical sampling site of a coarse gravel bar and channel gravel deposits is demonstrated.

3.1. Characterizing Grain Size

The modern riverbeds of the Iglesia basin fans are perennially dry, exposing a surface of gravel bar and channel deposits. Their beds comprise a mixture of gravel and sand, where sand becomes increasingly dominant in the downstream reaches of each fan. Exposed river banks along the incised channels reveal no evidence of surface coarsening. We characterized the size distribution of the coarser-than-sand "gravel" fraction ($>$ 2 mm) on the bed surface, every ~ 3 km along a mainstream, from the catchment mouth to fan toe. Our first sample site, X_0, is located ~ 3 km upstream of the fan apex, and the fan toe is defined either as a gravel-sand transition (fans 2 and 3), identified as a reach almost exclusively composed of sand ($>$ 95%) with only limited patches of fine gravel, or as a confluence with the axial drainage system (fan 1). Sampling was performed systematically upstream of any tributary influence, so as to minimize the impact of capturing extreme local variability in grain size (Rice & Church, 1998). A total of 10 localities were sampled on fans 2 and 3, and 12 localities were sampled on fan 1.

Photographic grain size analysis was used, consistent with the methodology of Attal and Lave (2006), to characterize the size distribution of gravel on the bed surface at each site. High-resolution photographs, taken vertically over the bed surface with an 80-mm-wide angle lens, sampled an area ~2 × 3 m, after cropping of the distorted edges of the image. A size distribution of 100 clasts was measured from each photo by overlaying an equally spaced grid and measuring the long axis of each clast beneath a cross hair. The spacing of grid nodes was set at least greater than the upper quartile of clasts sizes; the presence of boulders in the sample meant the largest clasts could fall under more than one grid node. To attain a sample best representative of the bed surface composition, we compensate for the greater volumetric significance of larger clasts, relative to smaller clasts, as highlighted by the voidless cube model of Kellerhals and Bray (1971). The volume of the sample is considered the particle dimension normal to the bed and, following the methodology of Attal et al. (2015), large clasts covering n cross hairs were counted n times.

To reduce sampling bias toward coarser or finer areas of the river bed, a representative gravel bar and channel deposit were sampled individually at each sample site. The size distributions derived for each site were subsequently merged into a composite single size distribution, where the relative contributions of gravel bar and channel deposits were scaled by in situ field estimates of their relative percentage cover at each site (Bunte & Abt, 2001).

The uncertainty in our grain size measurements and in our handling of the data cannot be calculated without a prior knowledge of the true grain size population. We assess the precision and potential bias of our approach to determine appropriate margins of error. Recounts of photographs find that the distributions are reproducible and a comparison of the distributions with in situ pebble counts, sampled along a measuring tape, indicate that the size distributions captured by the photographic technique provide a representative sample of the bed surface (see the supporting information). The ratio of the long and intermediate axes of clasts measured from the photographs does not change as the packing structure of the bed varies, indicating that clast exposure has a negligible impact on measurement precision, in this setting. As our sample size was limited by the diameter of clasts being measured, we predict the absolute precision in locating the D_{50} and the D_{84} of the parent population by extrapolating precision estimates for lognormal distributions, with similar standard deviations, from Rice and Church (1996). They estimate that both percentiles can be located with an absolute precision of ±0.84 mm for a sample size of 100 clasts. We establish that the most significant source of error in our data sets stems from our field estimates of the ratio of gravel bar to channel deposit coverage at each site. In the field, several workers made estimates of this ratio and were in general agreement to the nearest 10%. We recalculate the D_{50} of the final size distribution when the ratio of gravel bar to channel deposit is modified by 10%. We apply these two scenarios as sample error estimates on our D_{50} measurements and find that they are roughly equivalent to the D_{45} and D_{55} of each distribution.

3.2. Quantifying Sediment Source Contributions

To estimate the volume of sediment sourced from reworking of the fan itself, we make a first order assumption that the modern channels on each of the fans experience coeval incision and have incised into a spatially uniform fan surface over 10 kyr. This assumption is supported by field observations of the modern channels on all fans being entrenched 0.7–2 m into the surface mapped to be early Holocene in age. We apply 10 kyr as the maximum age for the recent surface and therefore estimate a minimum recycled volume. We use Google Earth Landsat images at ~30-m resolution to measure the width of the modern river channel at 1-km intervals downstream and apply field measurements of channel depth to calculate the volume of sediment that is currently missing.

For each of three fans, ArcGIS spatial analyst tools were used to delineate two types of catchments that supply sediment to the fans (see Figure 2). The first are primary catchments, which are delineated by the drainage network upstream of our first measurement site (X_0). The second are tributary catchments, which delineate the parts of the drainage network that feed sediment laterally into the active channel on the fan. Their outlets are defined where channels leave the confines of their bedrock valley. We used zonal statistics to calculate the area and maximum relief of each catchment.

The rivers here are not gauged so we do not have direct constraints on sediment fluxes from the source catchments. There are, however, well-established relationships between sediment flux (Q_s), basin area (A), maximum relief (R), and water discharge (Q) that can be used to provide first-order estimates of sediment flux generated by a catchment. Building on these relationships, other geologic, climatic, and geographic controls can also be factored in to improve Q_s predictions. Using a regression analysis of 488 rivers worldwide, Syvitski and Milliman (2007) demonstrate that 96% of the global variation in suspended sediment flux exported from a river's mouth can be accounted for when geologic, climatic, and geographic influences are factored in to relatively short-term (±30-year) estimates of sediment yield. We apply the following version of their so called "BQART" model to each delineated catchment feeding the Iglesia basin fans, to obtain a first order estimate of, Q_S.

$$Q_S = 2\omega BQ^{0.31}A^{0.5}R \tag{3}$$

Here Q_S is in MT/year when the unit conversion factor $\omega = 0.0006$, Q is in km^3/year, A is in km^2, and R is in km. B is a term that scales with glacial erosion (I) and lithology (L) and expands to $B = IL$. We derive Q for each drainage area using observed mean annual precipitation between 1960 and 1990 from the WorldClim database. As catchment average temperature values are ≤ 2 °C, a temperature at which the linear relationship between sediment yield and decreasing temperature breaks down (Hales & Roering, 2007), we follow Syvitski and Milliman's (2007) model for cold catchments. After Syvitski and Milliman (2007), $L = 1$ is appropriate for source lithologies that include hard plutonic and volcanic rocks. Glacial erosion, I, is defined as $(1 + 0.09A_g)$, where A_g

is the percentage of total catchment area that is glaciated. We convert annual BQART Q_S estimates to a longer term, volumetric flux in $m^3/10$ kyr, assuming 2.7 g/cm^3 and 30% porosity. Dividing the BQART Q_S estimates by the respective catchment areas, we are then able to compare denudation rates to those reported in the literature.

In estimating long-term sediment fluxes, we embed an assumption that glacial cover and precipitation rates have remained constant over the last 10 kyr. To take into account the impact of extreme events and climate variability, we considered modern and mid-Holocene climate scenarios, using mean annual and maximum precipitation data from CNRM-CM5 Earth system climate model (Voldoire et al., 2013), downloadable from the WorldClim database (Hijmans et al., 2005), and variable glacial cover. We find, however, that the uncertainty in estimating Q_S due to flux variability is significantly lower than the uncertainty in estimating the percentage of the load that is transported as bedload and further, in estimating the proportion of the bedload flux that is stored on the fan over geomorphic timescales. Globally, bedload is estimated to make up 10–70% of the total flux exported from catchment areas $<1,000$ km^2 (Pratt-Sitaula et al., 2007; Turowski et al., 2010). To estimate the bedload proportion of the load exported to the Iglesia basin fans, we multiply the first order BQART flux estimate by 40%; the average bedload proportion reported in the literature (Pratt-Sitaula et al., 2007; Turowski et al., 2010). We then calculate a range of uncertainty on these first-order estimates for when the bedload flux composes 10 and 70% of the BQART flux.

Using these approaches, we identified and estimated the sediment flux contributions from (i) the primary catchment, (ii) the tributary catchments, and (iii) fan recycling for each of three fans under consideration.

3.3. Quantifying Sediment Dynamics

Fedele and Paola (2007) demonstrate that the rate of change in the mean grain size over a distance downstream is a function of the spatial distribution of sediment mass extracted by size selective deposition. Here we exploit their methods for collapsing self-similar gravel size distributions and apply their self-similar solution for approximating the uniform fractionation of gravel downstream.

We first calculate the rate of downstream grain size fining on each fan using Sternberg's exponential function of the form:

$$D_x = D_0 e^{-\alpha X} \tag{4}$$

where D_0 is the predicted input median grain size to the river, α is the fining exponent, and X is the downstream distance (Sternberg, 1875). As a simple test for scale invariance, we test whether the local standard deviation, σ, decreases exponentially downstream at a rate similar to the mean, $\overline{D}$ (Paola, Heller, & Angevine, 1992; Paola, Parker, et al., 1992) by calculating the coefficient of variation, C_v of the grain size distributions:

$$C_V = \frac{\sigma(x*)}{\overline{D}(x*)} \tag{5}$$

If the gravel deposits are scale invariant, and therefore self-similar, the C_V is relatively constant for any downstream distance, where distance is normalized by the length of the depositional system, x^*. In this case, Fedele and Paola (2007) show that a similarity variable, ξ, can be derived of the form:

$$\xi = \frac{D - \overline{D}(x^*)}{\sigma(x^*)} \tag{6}$$

where D is the size of each individual grain in a distribution. If self-similar, the shape of the gravel size distribution at any downstream distance along the length of the fan will be the same when scaled by ξ. This form of ξ has previously been successful in transforming field data in a range of fluvial settings (D'Arcy et al., 2017; Duller et al., 2010; Seal & Paola, 1995). We derive ξ for each size distribution and then for each size distribution transformed into $\log_{10}(D)$. We test the normality of the distributions using a one sample Kolmogorov-Smirnov test.

To statistically compare the similarity between ξ distributions on each fan, we perform a Kolmogorov-Smirnov two sample test. The maximum difference or supremum, sup, between two probability distributions, $F_1(i)$ and $F_2(i)$, with sample size n and m, respectively, is calculated:

$$d_{n,m} = \sup_i \left(F_{1,n}(i) - F_{2,m}(i) \right) \tag{7}$$

The null hypothesis, which states that the two distributions are the same, is rejected if the test statistic d is larger than a critical d value for the given sample size and a significance level, α, calculated as

$$d_{n,m} > c(\alpha) \sqrt{\frac{n+m}{nm}} \tag{8}$$

We accept the distributions are the same with a significance level, α, of 5%, which, given the large sample size, is equivalent to $c(\alpha) = 1.36$ when:

$$c(\alpha) = \sqrt{-\frac{1}{2} \ln\left(\frac{\alpha}{2}\right)} \tag{9}$$

We compare all distributions on each fan and report the percentage of comparisons that are statistically similar. A fan can be described as self-similar if this percentage is appropriately large.

Assuming clast sorting by size selective deposition, we apply Fedele and Paola's (2007) relative mobility function J, (equations (1) and (2)) to reconstruct the fractionation of relative grain sizes between the transportable load and the substrate. We use an iterative least squares regression to attain a best fit for J to the average ξ distribution derived for each fan. As c_g ought to be a small constant for our three fans, we fix c_g and allow dependant variables a_g and b_g to vary through iterative refinement. We attain a best fit with 95% confidence bounds. Variable c_g is not well constrained in the literature. From the ACRONYM model runs, Fedele and Paola (2007) derive a c_g of 0.15, whereas a c_g of 0.08 was back-calculated for data published for the North Fork Toutle River, Washington (Seal & Paola, 1995). For the ξ distributions derived from the original size data, we derive a best fit for J when c_g is fixed at 0.15, as this value best describes the asymptote of the falling limb. For the ξ distributions derived from the logarithm of the size data, the c_g scales closer to 0 and is best approximated by a low but finite c_g of 0.01.

J quantifies the mobility of different clast sizes based on their relative proportion in the substrate and, therefore, communicates the probability that each clast size will be held in transport or will be deposited in the substrate. We observe how J varies with ξ on each fan to characterize the mobility of the substrate. Further, we observe how J varies with physical grain size, D (mm), when D is back calculated from ξ using the average mean grain size and standard deviation on each fan.

$$D = \xi\, \sigma + \overline{D} \tag{10}$$

Using this approach we are able to compare bedload mobility estimates across different fans. In addition to the three fans described in this study, we compared the relative mobility curves of two fans in northern Death Valley, California. Following the same modeling procedure, we analyzed grain size data published by D'Arcy et al. (2017) for a modern surface and a 70-kyr surface on two neighboring fans, the Moonlight and Backthrust Canyon fans. This data set provided an opportunity to compare bedload mobility estimates between systems with different boundary conditions and allowed a comparison of more-recycled versus less-recycled fans.

4. Results

Distinct morphological differences exist among the three adjacent fans studied. Fan 3 stands out in having a braided channel network that becomes more distributive downstream across the center of the fan, so that the active surface widens toward the fan toe. On fans 1 and 2, the braided channels are focused toward the northern edge of the fan and they occupy a narrow valley downstream. These morphological differences influence the area of fan being recycled, allowing us to investigate the sensitivity of deposited grain sizes in a range of geomorphic settings.

4.1. Sediment Flux

Our estimates of the sediment flux available for export to each fan over 10 kyr are in the order of $10^8\ \mathrm{m^3}$ and translate to average denudation rates of ~0.06 mm/year. The southernmost fan, 2, is estimated to export

Table 1
Summary of Catchment Characteristics and Sediment Fluxes Derived for Each Fan System

	Fan 1	Fan 2	Fan 3
Total catchment area (km^2)	903	302	343
Fan area (km^2)	511	170	170
Maximum relief (km)	3.51	3.46	2.71
Discharge (m^3/s)	6.53	2.2	2.26
Catchment average temperature ($^{\circ}C$)	−2.2	−1.1	−3.1
Glacial cover (%)	1.91	2.63	0.44
BQART model sediment flux estimate ($m^3/10$ kyr)	5.14×10^8	1.97×10^8	1.48×10^8
Denudation rate (mm/yr)	0.06	0.07	0.04
Bedload flux to fan ($m^3/10$ kyr)	$2.06 \times 10^8 \pm 1.5 \times 10^8$	$7.89 \times 10^7 \pm 5.9 \times 10^7$	$5.91 \times 10^7 \pm 4.43 \times 10^7$
Bedload yield ($m^3/10$ kyr/km^2)	$2.3 \times 10^5 \pm 2.2 \times 10^5$	$2.6 \times 10^5 \pm 1.9 \times 10^5$	$1.7 \times 10^5 \pm 1.3 \times 10^5$
Recycled flux ($m^3/10$ kyr)	$4.2 \times 10^7 + 6.2 \times 10^6 - 3.9 \times 10^6$	$9.1 \times 10^6 + 3.6 \times 10^6 - 2.1 \times 10^6$	$5.3 \times 10^7 + 2.5 \times 10^6 - 1.8 \times 10^7$

1.97×10^8 $m^3/10$ kyr and has the highest denudation rate, 0.07 mm/year, fan 1 exports 5.14×10^8 $m^3/10$ kyr and has a denudation rate of 0.06 mm/year and the northern most fan, 3, has the lowest export, 1.48×10^8 $m^3/10$ kyr and the lowest denudation rate, 0.04 mm/year. This relatively low rate of erosion is analogous to millennial catchment averaged erosion rates derived from cosmogenic-nuclide and thermochronometric studies, which typically report values between 0.04 and 0.1 mm/year (Sepulveda et al., 2015). This gives confidence that the catchment characteristics derived (Table 1) provide reasonable estimates of sediment export to within an order of magnitude.

The proportion of the total Q_S exported as bedload is not expected to vary significantly across the mountain front, as catchment morphologies and rock types are alike. The error on the percentage bedload flux is likely systematic across the three catchments, allowing us to compare estimated bedload fluxes between sediment sources to first order. Assuming bedload is approximately 40% of the total sediment flux for all three fans, the percentage of Q_S introduced laterally into the river varies significantly between fans (Figure 3). Catchments that we identify as tributaries supply approximately half (~46%) of the total catchment bedload Q_S to fan 1. Tributaries supply ~18% of the total Q_S delivered to the active channel on fan 2, whereas tributaries supply the active portion of fan 3 with ~68% of the total Q_S. In Figure 3, we compare catchment bedload Q_S with the Q_S supplied by fan reworking. We estimate, despite its larger size, that fan 1 has reworked a volume equivalent to $38 \pm 86\%$ of the primary catchment bedload flux. Fan 2 also has a small recycled component, $14 \pm 6\%$ of the primary catchment bedload flux. On the other hand, for fan 3 we estimate that a much more significant flux of recycled sediment that is $285 \pm 97\%$ of the primary catchment flux. These systems uniquely provide a range of end-members to test how fundamental differences in sediment sourcing, impact grain size trends on fans.
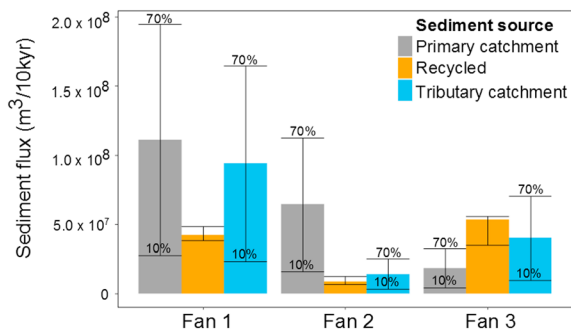

Figure 3. A comparison of the fluxes of sediment estimated to be delivered to each fan from primary and tributary catchments and from fan surface recycling. The catchment sediment fluxes are bedload fluxes, where bedload is estimated to make up 40% of the total exported Q_S. The error bars are systematic and represent 10 and 70% of the total Q_S exported as bedload. The error bars on the recycled fluxes record the uncertainty in measuring the width of the modern valley between Holocene terraces.

4.2. Sediment Sorting

In Figure 4, we present the cumulative frequency curves of each fan's grain size distributions alongside the cumulative frequency curves of the logarithmic size distributions. A one-sample Kolmogorov-Smirnov test (K-S test), detailed in the supporting information, demonstrates the cumulative frequency curves of the log size distributions are lognormal. This is important as it indicates that the shape of the distribution is not an artifact of the truncation by the 2-mm measurement cutoff. Furthermore, it demonstrates that the applied statistics, which assume normality, are suitable for this data set.

The cumulative frequency curves for all fans show a broad trend for distributions to become narrower and finer from fan apex to toe. This trend is most pronounced for fans 2 and 3, which have broader distributions at site 1 compared to fan 1, that is, at the fan apex where $x^* = 0$, denoted as X_0. The size distribution at X_0 on fan 2 is broader and coarser than fan 3: fan 2 has a D_{50} of 135 mm, a D_{84} of 350 mm, and a σ of 137 mm, compared with
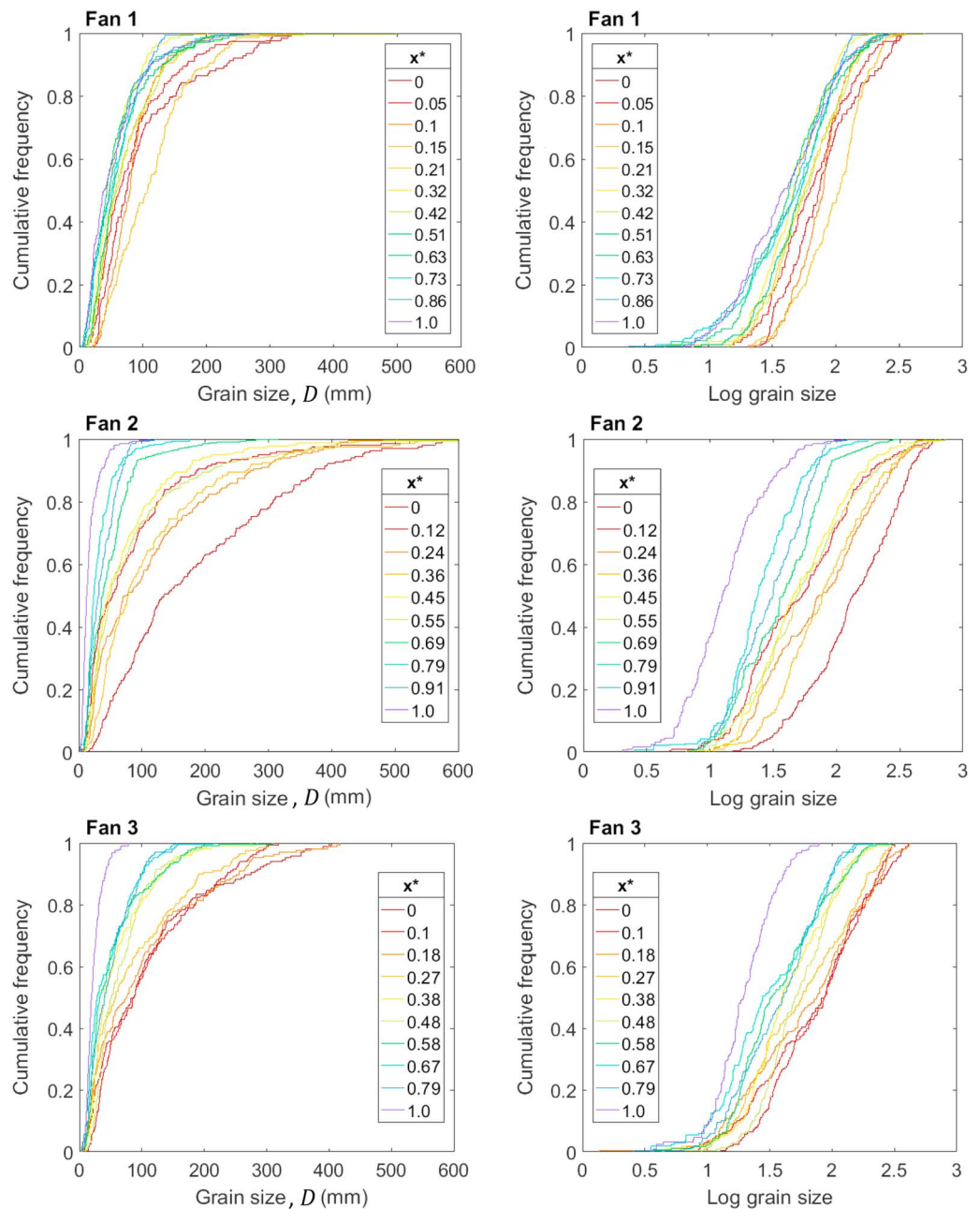
Figure 4. Cumulative grain size and log grain size distribution curves for each locality at their normalized distance downstream, x^*, on fans 1, 2, and 3, respectively. Each distribution curve is derived from the size distributions of 100 clasts counted on both gravel bar and in-channel deposits, and scaled for their at-site areal coverage (see methods).

86, 275, and 95 mm for fan 3, respectively. At the gravel-sand transition, site 10, the size distributions on both fans are similar and have a D_{50} of 13 and 19 mm, respectively; a D_{84} of 25 mm, and a σ of 14 mm. In contrast, the size distributions on fan 1 are more similar from apex to toe and have a less pronounced shift in grain size range or curve shape. The D_{50}, D_{84}, and σ of the size distribution at X_0 is finer than the other fans, 74, 175, and 75 mm, respectively, and the D_{50}, D_{84}, and σ at the confluence with the axial drainage system, site 12, is coarser, 39, 85, and 48 mm, respectively.

In Figure 5, the D_{50} and D_{84} of each distribution are plotted against its distance downstream for each fan. Exponential regressions provide a good fit for the broad fining trend on fans 2 and 3. Fan 2 has a fining exponent of -0.071 ± 0.036/km with an R^2 value of 0.77, and fan 3 has an exponent of -0.064 ± 0.02/km with an
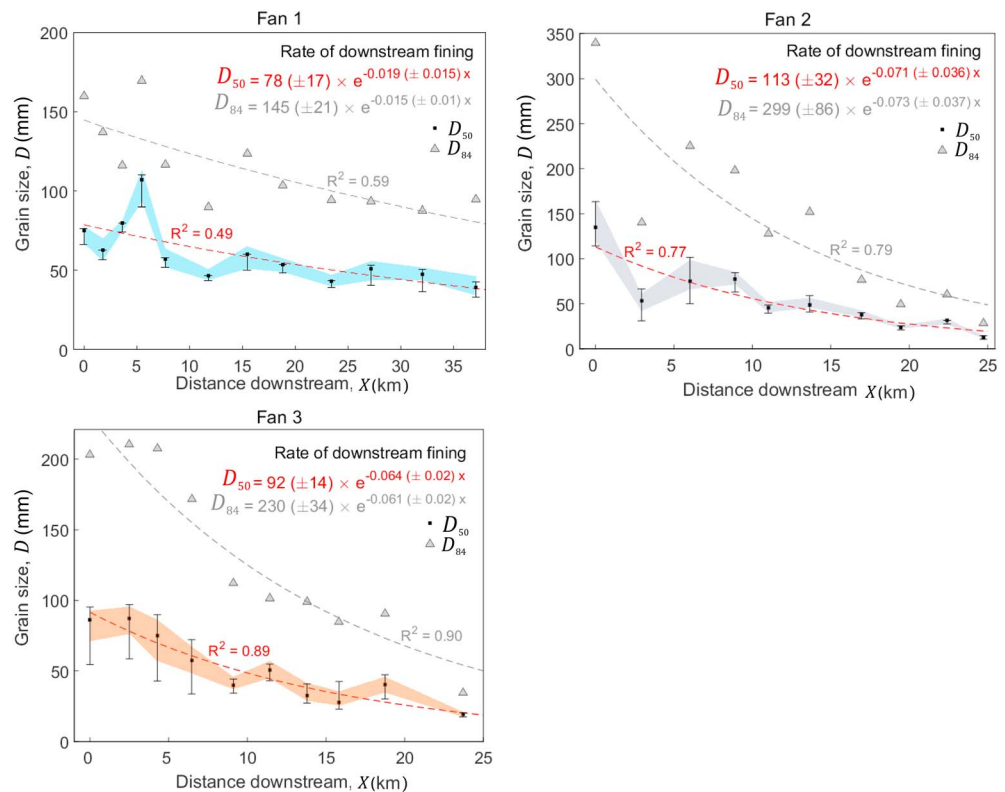
Figure 5. D_{50} and D_{84} grain sizes measured at each locality, plotted against distance downstream from the fan apex. The D_{45} and D_{55} percentiles are plotted as colored bands to demonstrate the spread of data about the median. These percentiles roughly correlate with the error bars, which highlight the potential measurement error. An exponential regression is fit to each data set, for which an R^2 value is given. The best fit regression equations are quoted with the 95% confidence intervals for the regression intercept, D_0, and the downstream fining exponent, in brackets.

R^2 of 0.89. The 95% confidence bounds of their least squares regressions overlap, indicating that fans 2 and 3 have rates of downstream fining that are statistically similar. The exponential regression derived for fan 1 has an R^2 value of 0.49, capturing the localized spike in median grain size in the upper fan. The fining exponent for fan 1 is less negative than the other two fans, -0.019 ± 0.015/km. The input grain size, D_0, derived from the regression at X_0, varies between fans: 78.8 ± 17 mm, 113 ± 32 mm, and 91.6 ± 14 mm for fans 1, 2, and 3, respectively. The D_{84} of the distributions on all three fans have exponential rates of downstream fining with exponents that are statistically similar to the rates of D_{50} fining. The fining exponents for D_{84} percentile on fans 1, 2, and 3 are -0.015 (± 0.01), 0.073 (± 0.037), and -0.061 (± 0.02)/km, respectively, which are within 95% confidence bounds of the least squares regression for the D_{50} percentile. The fits of the D_{84} exponential curves have higher R^2 values than the D_{50}; 0.59, 0.79, and 0.90, for fans 1, 2, and 3, respectively. The initial D_{84} at the fan apex is 145 ± 21 mm, 299 ± 86 mm, and 230 ± 34 mm, for fans 1, 2, and 3, respectively. The exponential fining is consistent with a downstream reduction in grain size, which is a necessity of the Fedele and Paola (2007) approach. However, it should be highlighted that while exponentials provide a reasonable fit to the data, fining is not monotonic; the curves average out substantial fluctuations in both D_{50} and D_{84} grain sizes, particularly in the upper reaches of each fan. Tributary confluences are focused in the upper reach of the fans and can be tied in space to these fluctuations.

4.3. Self-Similarity

The typical C_V range for self-similar gravel deposits identified in numerical experiments and field studies is between 0.7 and 1.0 (D'Arcy et al., 2017; Duller et al., 2010; Fedele & Paola, 2007; Seal & Paola, 1995). In Figure 6, C_V varies between 0.6 and 1.2 across the fans; however. this variation falls within the sensitivity limits of the ratio to $\pm 10\%$ measurement error in the mean and standard deviation. Fitting an exponential curve to
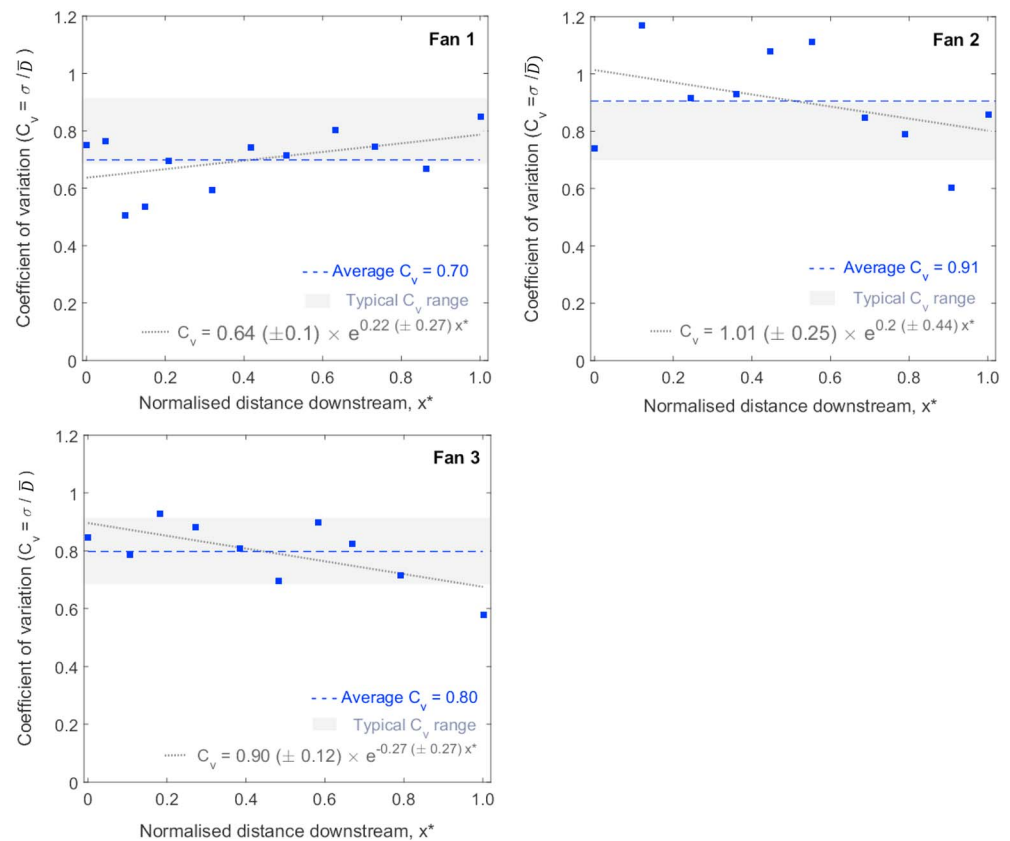
Figure 6. The coefficient of variation calculated for each site distribution, plotted against normalized distance downstream from the fan apex (X^*). The pale band highlights the range of C_V values typically observed in natural self-similar deposits and in hydraulically based fining models where sorting is controlled by grain size partitioning downstream (e.g., Parker, 1991; Seal & Paola, 1995). The dotted line highlights the average C_V for the respective fan. Average C_V values indicate that the deposits of fan 1 are most well sorted, with an average C_V 0.70 ± 0.2 and least well sorted on fan 2, average C_V 0.91 ± 0.3, and are intermediate on fan 3, average C_V 0.80 ± 0.2. There is no statistically significant trend in C_V downstream for any of the three fans.

the data on each fan, we observe downstream fining exponents with standard errors that are indistinguishable from 0: Fans 1, 2, and 3 have exponents 0.22 ± 0.27, -0.2 ± 0.44, and -0.27 ± 0.27/km, respectively, for regressions with R^2 values of 0.20, 0.15, and 0.41, respectively. With increasing distance downstream, the size distributions of gravel on each fan show considerable scatter with no statistically significant tendency to become better or less well sorted (cf. Miller et al., 2014). This allows us to apply a similarity variable in the form of equation (6).

The statistical similarity between ξ distributions, evident in Figure 7, is strong between ξ log distributions, which attain pass rates of 97, 92, and 100% for fans 1, 2, and 3, respectively. The ξ original distributions are less similar with pass rates of 82, 44, and 68%, respectively (Figure A1). Some of the variability captured in the original distributions could be attributed to measurement uncertainty as the similarity variable is sensitive to subtle changes in the mean grain size, particularly when $\xi_{(g)}$ is close to 0. The coarse tails of the distributions also introduce uncertainty, as the mean is sensitive to outliers. In Figure 7g, we also plot ξ distributions of landslide deposits sampled in Nepal, published in Attal and Lave (2006). The variability in the shape of the landslide size distributions is considerable and demonstrates that applying a logarithm to the data sets does not automatically force a collapse of the data into a single lognormal distribution. Furthermore, it highlights that the dominant influence fluvial sorting processes have in transforming the size distribution of landslide material they are supplied with (Allen et al., 2017; Roda-Boluda et al., 2018).

In its current form, J (equation (2)) accommodates ξ distributions that approach normality. As ξ employs the mean and the standard deviation as shape scalers, it is important that the size data are approximately
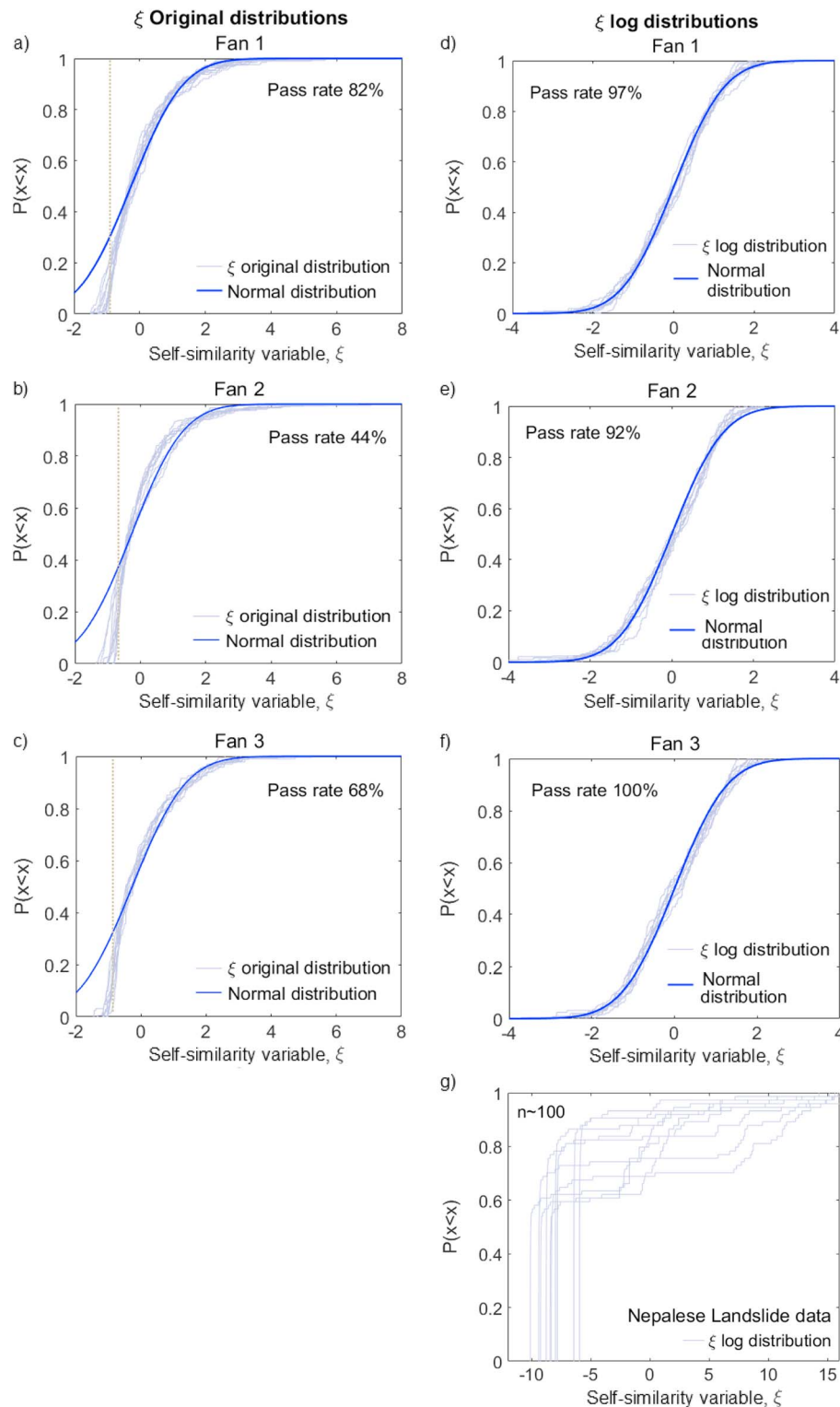
Figure 7. (a–c) Cumulative distributions of similarity variable, ξ, derived from each measured grain size distribution along the length of fan systems 1, 2, and 3, respectively. The grey dotted lines highlight the area of the distribution influenced by truncation. (d–f) Cumulative distributions of similarity variable, ξ, for the same data sets, derived after a logarithm is applied to the original size data. The solid blue distributions are reference normal distributions used to statistically test for normality in a one sample Kolmogorov-Smirnov test (see the supporting information). (g) The ξ log distributions derived from Nepalese landslide data, published in Attal and Lave (2006); these data do not overlap in ξ space. The statistical similarity between the alluvial fan distributions in a–f, as determined from a two sample Kolmogorov-Smirnov test, is summarized as the percentage of the distributions that are similar within a 5% significance. We report this value as a pass rate for each fan, where the Kolmogorov-Smirnov matrices are presented in the appendix.
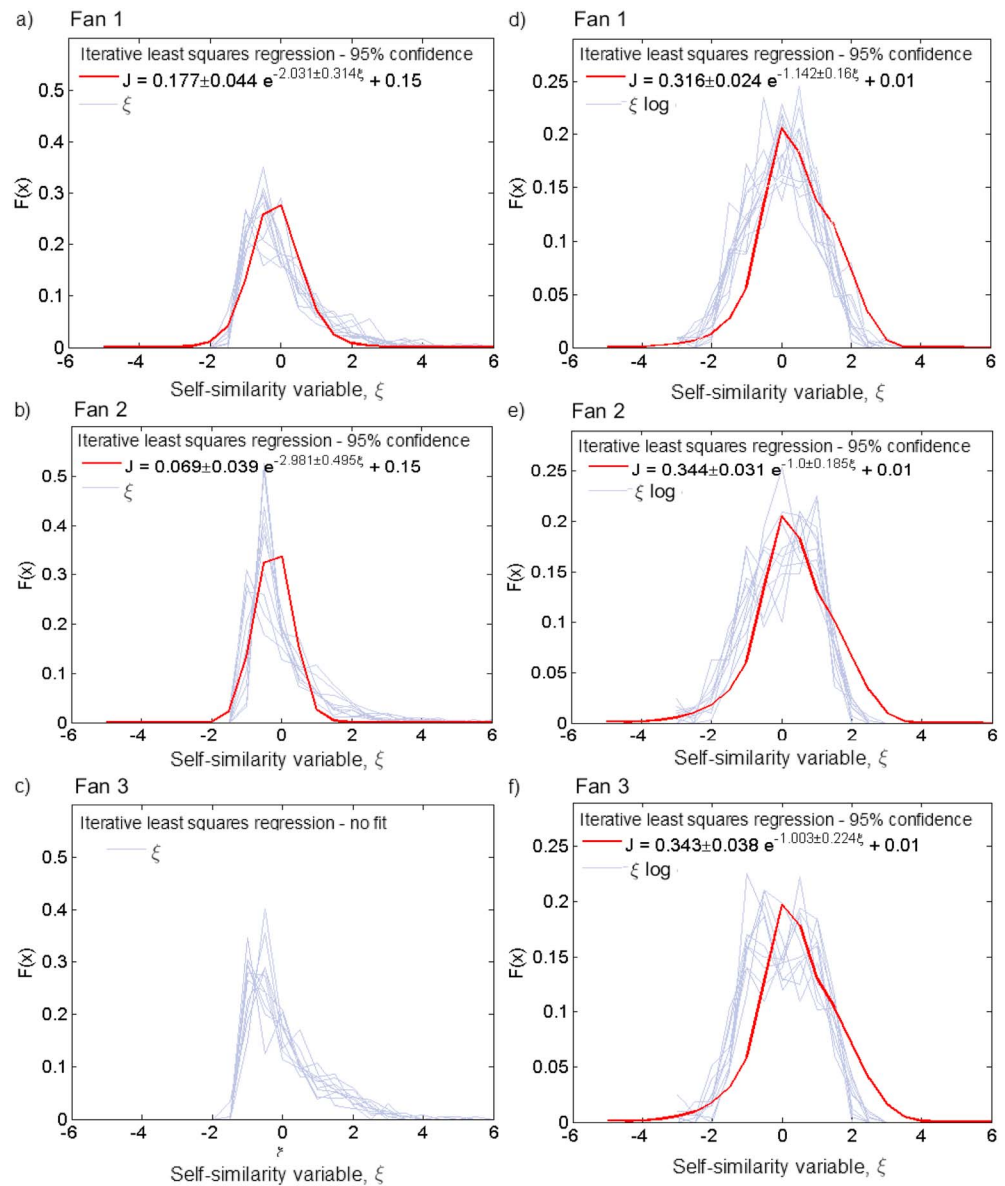
Figure 8. (a–c) Frequency distributions of similarity variable, ξ, derived from each measured grain size distribution along the length of fan systems 1, 2, and 3, respectively. The red distribution is our fit of relative mobility function J to the ξ distributions, attained using an iterative least squares regression of equation (2) when c_g is fixed at 0.15. This method failed to find a statistically significant fit for fan 3, and therefore, we omit the model fit from the analysis. The statistical fit with 95% confidence bounds is reported. (d–f) Frequency distributions of similarity variable, ξ, derived from each measured grain size distribution after a logarithm is applied. The red distribution is our fit of relative mobility function J to the ξ log distributions, attained using an iterative least squares regression of equation (2) when c_g is fixed at 0.01.

normally distributed if they are to be effectively transformed. Plotting ξ distributions incrementally, in Figure 8, we observe the original data peak around −0.5 to −1 with a short negative limb, truncated by the sampling technique, and a strong skew on the positive limb. $\overline{D}$ is equivalent to $\xi = 0$ and as the ξ transformation assumes that the size distribution is normal, the data would be expected to peak around 0. For the original distributions, the ξ data peak is shifted to the left, indicating that the long coarse tails of the distribution are significant in skewing $\overline{D}$ so that ξ is less effective in describing the shape of the data. When the ξ distributions are derived from the logarithm of the size data, the data are normally distributed so that the significance of the positive skew in the coarse tail is reduced, relative to the finer end of the distribution. The symmetry of the distribution indicates that ξ has more effectively transformed their
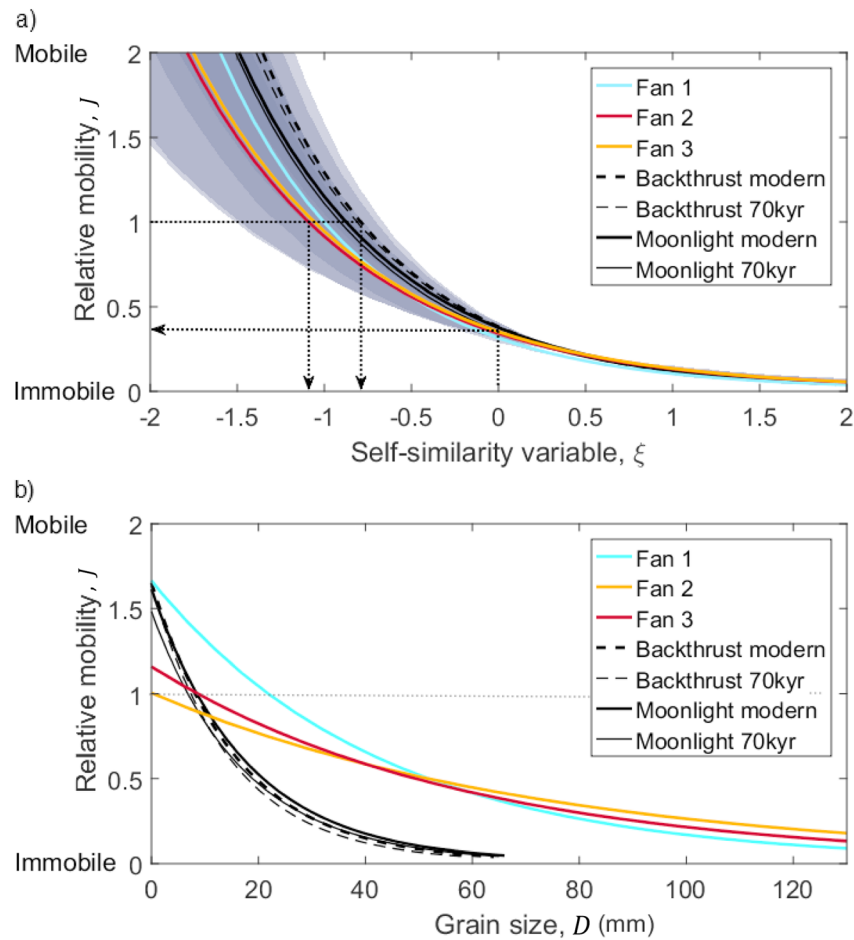
Figure 9. (a) The relative mobility, J, of the nondimensionalised self-similar grain size, ξ, modeled in Figure 8, is plotted as a curve for each of three Iglesia basin fans. Additionally, we include relative mobility curves that we derive for modern and 70-kyr surfaces on two small fans in Death Valley, California, using data published in D'Arcy et al. (2017). (b) The relative mobility, J, of clasts sizes, D, when clast size is calculated from ξ using the average median grain size and standard deviation on each fan system, respectively (equation (10)).

shape, and the data peaks are observed to collapse approximately over 0, within the range of −1 to 1. A one sample K-S test, included in the supporting information, demonstrates statistically that all log distributions are normally distributed and the two sample K-S test demonstrates log distributions on each respective fan are statistically similar. Apparent variability between distribution shapes in Figure 8 is therefore not statistically significant and largely a function of the bin width chosen to display the data and minor site specific deviations. In Figure 8, we include the fit derived for J (red), when the distributions could be effectively modeled. For ξ distributions derived from the original size data, a statistical fit for J, when c_g is set to 0.15, fails to provide a good approximation of the data peak and the skewed positive tail. The goodness of fit for J decreases from fan 1 to fan 3, where fan 3 cannot be modeled by J without substantial error. Applied to the ξ log distributions, a good fit for J can be derived for all three fans. By applying a logarithm, resolution in the positive coarse tail of the distribution is lost and the value to which the model curve becomes asymptotic, that is, c_g is required to be close to 0. This communicates that the model J fit is less sensitive to the initial motion conditions and that the probability that any sized clast will be immobile is low. With this approach, values derived for a_g are 0.32 ± 0.02, 0.34 ± 0.03, and 0.34 ± 0.04 and for b_g are 1.14 ± 0.16, 1.00 ± 0.18, and 1.00 ± 0.22 for fans 1, 2, and 3, respectively.

As relative mobility function J is a probability ratio of a particular grain size class being present in transport and stored on the bed surface (equation (1)), when J is equal to 1, the respective clast size is equally likely to be in the substrate as in transport. In Figure 9a, we plot J against ξ and observe the section of the curve

that falls below $J = 1$ and their accompanying x axis values. This describes grain sizes that are increasingly more likely to be in the substrate than in transport and are consequently less mobile.

The model curves derived for all alluvial fans fall within the margin of statistical error. Their mobility is low; the mean clast size ($\xi = 0$) is ~60–70% more likely to be in the substrate than in transport. As such, the clast sizes that have a 50% probability of being entrained (i.e., when $J = 1$) are much finer than the mean, between -1.5 and $-0.8\ \xi$.

Figure 9a also plots the relative mobility curves derived for two smaller fans in Death valley, California, from data published in D'Arcy et al. (2017). The Moonlight and Backthrust Canyon fans are both ~ 6 km in downstream length, though have distinctly different morphologies. D'Arcy et al. (2017) describes the Moonlight fan as having 40 m of fan head incision into an older 70=kyr terrace, where they estimate that the volume of material that has been reworked is of the same order of magnitude as the catchment supply. Incision into the Backthrust Canyon fan is more subdued, where only a few meters of down-cutting is observed. These Death Valley fans and their respective 70-kyr surfaces plot to the right of the Iglesia basin fans and have a larger ξ when $J = 1$; however, all fans fall within the margin of statistical error, indicating that these differences are not statistically significant.

In Figure 9b, the estimated relative mobility curves for all these fans are plotted against dimensional grain size in millimeters, exploiting equation (10). The fans from Death Valley plot away from the Iglesia basin fans in this dimensional grain-size graph, predominantly because their measured mean grain sizes for the fan surfaces are different, although the shapes of their J, ξ functions overlap with the Argentine fans studies here. We observe that fan 1 has the coarsest grain size for when $J = 1$, ~22 mm, where all other fans have a $J = 1$ of <10 mm. The size range of clasts deposited on the Death Valley fans is much narrower, ~ 60 mm, than the Iglesia basin fans, > 120 mm. The substrate of the Death Valley fans could therefore be interpreted as more mobile because a greater proportion of the distribution is likely to be in transport. The greater mobility of fan 1's substrate, despite the wider grain size range, may be tied to a larger proportion of coarser grains being transported.

5. Discussion

The size distribution of gravel deposited on a river bed surface ought to preserve information about the river's dominant sorting mechanism (Parker, 1991). Applying a self-similar transfer function, we find, although the size distributions are physically diverse, the relative mobility of clasts deposited on five arid alluvial fans across two study areas, is statistically similar. This is evidence to suggest that size selective deposition is the dominant sorting mechanism on these alluvial fans. We explore the extent to which these rivers can be described as self-similar and what impact sediment recycling has in influencing this sorting mechanism.

5.1. Self-Similarity of Grain Size Distributions

Identifying a self-similar form in grain size distributions first requires the use of appropriate statistics that can effectively transform the shape of a distribution into a nondimensionalized space. The similarity variable used in this paper's methodology requires the distributions to approach normality. The similarity variable proposed by Fedele and Paola (2007) does a good job of collapsing our grain size data onto a single curve, although it does not completely describe our original size distributions due to a positive skew that is to some extent augmented by the truncation of the negative limb at the measurement limit for gravel. However, the normal distribution requirement can be fulfilled through a transformation of the grain size data into log space. By applying a log to the data, the significance of the positive skew is reduced and the similarity variable effectively describes the data so that the peak ξ distribution approximately correlates with 0.

The similarity between ξ log distributions is demonstrably strong. The two sample K-S test identifies a statistical similarity, with 5% significance limits, greater than 90% for all fans. The similarity between ξ distributions derived from the original data is more variable between fans; this deviation from similarity is greater than our measurement error and can be correlated with variability in the coarse, positive tails of the distributions. The coarse tails of the distributions, described by the D_{84} or D_{90}, are the least well-resolved percentiles and given the limited sample size, are subject to sampling bias (Ferguson & Paola, 1997). The less frequent, coarsest clasts in the riverbed population are expected to sometimes be sampled within our data set, though the extent to which this impacts variability in the tails of the distributions will depend on local variance on the

bed surface. Since the tails are suppressed when a log is applied to the size data, observing the improvement in similarity once the data are transformed provides useful information on the importance of the tails. The log transformation has the most significant impact on similarity for fans 2 and 3, suggesting that coarse tails were significant in causing a deviation from similarity. The similarity between the original size distributions of fan 1 is strong with or without a log transformation; these distributions also have a less substantial coarse tail. We observe that the magnitude of the sampling bias and the deviation from similarity is correlated with the presence of greater populations of larger clasts on the bed surface.

5.2. Sediment Mobility on Alluvial Fans

The relative mobility curves we derive for alluvial fans describe a substrate systematically enriched in coarse clasts that have a low mobility, where the mean grain size of the substrate is ~60–70% more likely to be in the substrate than in transport. This is in contrast to the findings of Fedele and Paola (2007) for the gravel bed, North Fork Toutle River, Washington, where the mean grain size of the substrate was found equally likely to be in transport as in the substrate. Using experimental data, Toro-Escobar et al. (1996) observed bedload fractions systematically finer than surface fractions in aggrading rivers, where the lower mobility of coarser grains resulted in their over-representation in the substrate with respect to the more mobile, finer grains. Such dynamics are consistent with our findings for the Iglesia fans; the size distribution on the surface of an arid alluvial fan is coarser than the size distribution transported as bedload. Toro-Escobar et al. (1996) also observed that a shift toward equally mobile conditions encouraged the surface to become biased toward the size distribution of the bedload (Ferguson et al., 1996; Haschenburger & Wilcock, 2003). This profile would fit well with the more mobile bed of the North Fork Toutle River where a greater proportion of bed material is mobilized regularly by high magnitude flows.

The heavy tails of the Iglesia riverbed gravels could also support experimental studies of partial transport in equilibrium gravel bed rivers (Wilcock & McArdell, 1993). There is no evidence of surface coarsening, typical of perennial equilibrium rivers (Dietrich et al., 1989); however, the fact that the Iglesia rivers are ephemeral and dominated by intense, short-lived events likely limits the exposure of the beds to the low flows responsible for winnowing the finer clasts (Laronne et al., 1994). Coarse clasts that are introduced into the river by incision into coarser surfaces or by extreme events could remain immobile or have a very low likelihood of entrainment under more subdued environmental conditions. The presence of immobile grains on the bed surface has been shown experimentally to directly influence the rate and size of vertical sediment exchange between the bedload and the substrate (Wilcock & McArdell, 1993, 1997; Wilcock & Southard, 1989). Wilcock and McArdell (1997) demonstrate, theoretically, that the presence of immobile grains should cause a systematic deviation from similarity in the fractional transport rate so that bankfull dimensionless shear stress of the river is not constant downstream. This theory recognizes that the entrainment frequency calculated for the whole bed will differ significantly from the entrainment frequency of those grains that are actively transported under prevailing flow conditions. Therefore, a deviation from self-similarity in deposited grain size distributions could be attributed to a significant proportion of coarse immobile grains on the bed surface. The impact of immobile grains on first, the similarity between size distributions, and second, the relative mobility of clast sizes, should be significant here.

Our results highlight fan 1 as having a greater mobility of coarser grain sizes than fans 2 and 3: the grain size with an equal likelihood of being entrained as being stored on fan 1 is 22 mm compared with <10 mm on fans 2 and 3. As fan 1 is twice as large as fans 2 and 3, this difference could be indirectly related to time-averaged flow strength, as this variable controls the proportion of the bed that is mobilized in a flow event.

5.3. Lateral Inputs and Sediment Recycling

Estimates of the sediment fluxes involved in each sediment routing system, which indicate the potential for sediment recycling to buffer deposited grain size trends, vary significantly between the three fans. Fan 3, whose modern channel is actively incising into a substantial area of its surface, has recycled a volume of material that is of a similar order of magnitude as the sediment flux delivered by its catchment. This is in contrast to fans 1 and 2, where incision has been limited to a smaller area of the fan and recycled volumes are significantly lower than the upstream catchment flux. Fan 3 also receives the highest proportion of its catchment sediment flux from its tributary catchments, making lateral inputs of sediment important for the mass balance of the system. These marked geomorphic differences can be correlated with deviations from self-

similarity between untransformed distributions and the error in fitting J to these distributions. The most recycled fan, 3, deviates from self-similarity, and an appropriate J fit to the original data cannot be found, implying that the sorting of bedload according to J cannot be inverted from the original size distribution of clasts on the bed surface. Our ability to fit J to fan 3's data after a logarithmic conversion highlights that the shape of the tails are integral for the fit to the untransformed distributions, and that by reducing the sensitivity of the fit to the tails with the log transformation, all fans maintain very similar bedload mobility profiles. As such, we find that the two fans that have similar catchment sediment fluxes and bedload mobility profiles have statistically similar rates of downstream fining.

The rates of exponential grain size fining average substantial fluctuations in the median grain size downstream. Tributaries have been previously observed to disrupt downstream grain size finings trends (Rice, 1999; Rice & Church, 1998). The fluctuations observed on the Iglesia fans are focused in their upper reaches and correlate in space with the zone of tributary confluences. However, there is no systematic deviation in the similarity of the substrate size distributions here; therefore, we indirectly observe that the change in volume and size distribution of the sediment load downstream of a lateral input does not influence the relative mobility of bedload estimated in the river. Sediment supply is thought to have an important control on the degree of bed surface coarsening in perennial rivers (Dietrich et al., 1989); however, the additional lateral sediment inputs into the ephemeral rivers of the Iglesia fans are not observed to have this effect. This finding is supported by several experimental data sets that have found; following perturbation by gravel pulses, the beds of low sloping rivers restabilize with a size distribution approximately equivalent to the unperturbed bed (Sklar et al., 2009; Venditti et al., 2010a, 2010b).

5.4. Implications for Quantitative Modeling and Environmental Interpretation

Detecting self-similarity among deposited gravel size distributions of such large, natural rivers is significant. It indicates that a steady state of bedload mobility can be achieved even in systems that are not strictly linear in transferring sediment from a single point source to sink. The Iglesia basin fans are generally self-similar despite being fed by a number of lateral sources downstream and irrespective of the degree of surface recycling. This suggests that autogenic behaviors that operate during the deposition of stratigraphic units do not generate enough noise to override the dominant sorting mechanism. We do, however, recognize the importance of immobile grains that are a common characteristic in low mobility, gravel bed rivers. The residence time of the coarsest clasts on the river bed depends on discharge variability, and therefore, the frequency of higher magnitude events, capable of mobilizing a large proportion of the bed, is highlighted as a control on the time taken for the river to adjust and reequilibrate to the modern sediment load being transported through the river.

For the application of relative mobility function J in a grain size fining model, the impact of coarse immobile grains on the mobility of bedload in these rivers may be minimal and can be modulated by how the data is treated. The largest source of error that may arise from applying a self-similar grain size fining model to original data may be related to the variability in median grain size downstream. For example, the exponential fining trends, derived for the fans in this study, average out substantial variations in median grain size in the upper fan. This gives uncertainty as to the caliber of total sediment volume supplied to the fan. Future work ought to investigate the errors associated with inverting and predicting the input grain size, the pattern of subsidence, and the volume of sediment supplied, from measured grain size fining trends with known climatic and tectonic boundary conditions.

6. Conclusions

We demonstrate, in natural, transport-limited rivers with low substrate mobility, such as those on arid alluvial fans, self-similarity in deposited gravel size distributions is detectable and can be an effective way to model size-selective transport dynamics. In a natural field setting, we quantify observable differences in the erosional dynamics on three alluvial fans by comparing their relative sediment flux contributions from respective catchments and from reworking of their Holocene surfaces. Our first-order estimates of their catchment supplies are on the order of 10^8 m^3/10 kyr and are consistent with catchment average erosion rates of ~ 0.06 mm/year; comparable to millennial rates published for the region. The flux of reworked sediment varies significantly between systems; one fan stands out in having a reworked flux that is ~285 ± 97% of the estimated primary catchment supply of bedload, compared to <40% on the other two fans. Collecting gravel size data for the
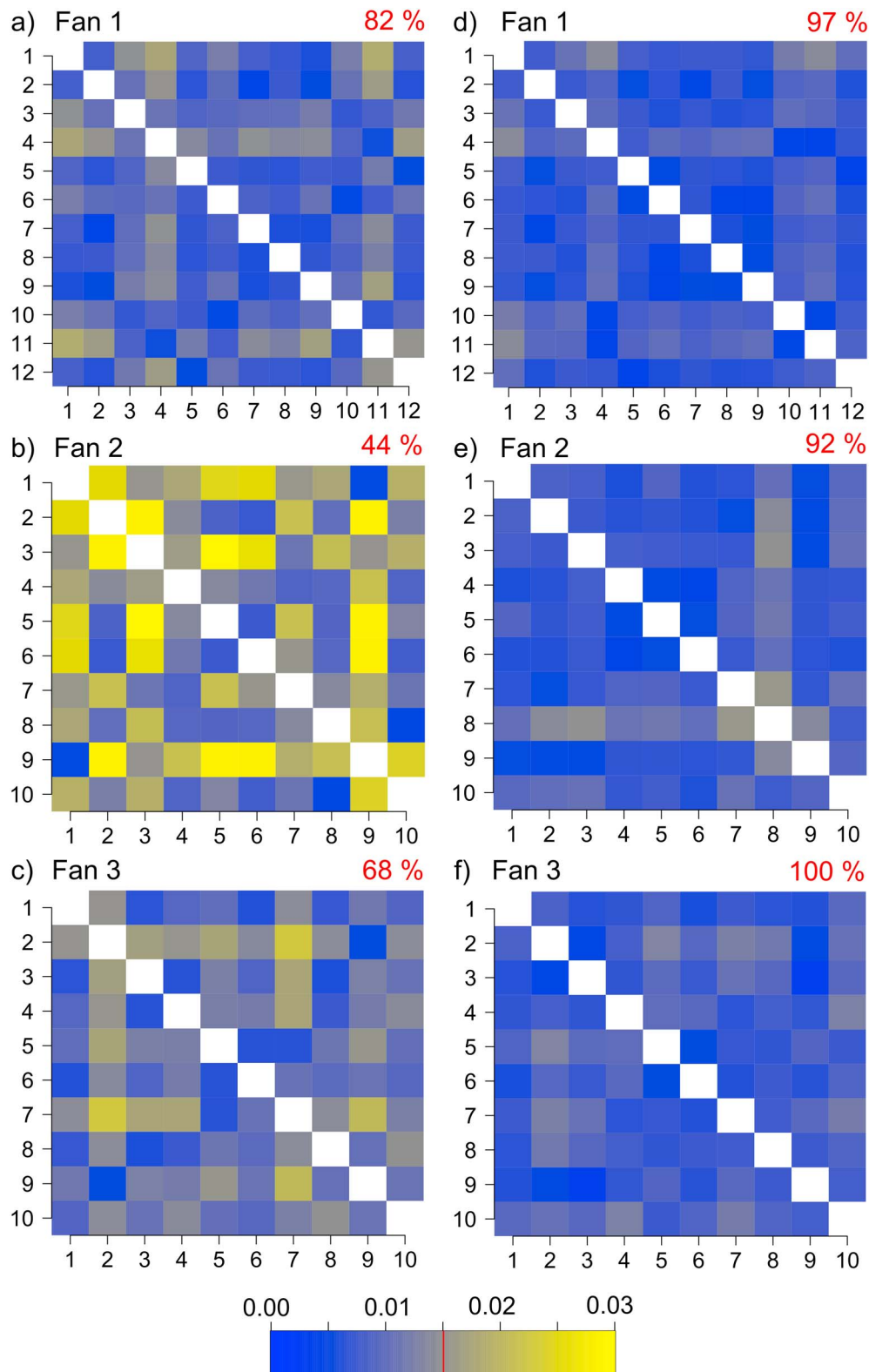
Figure A1. Kolmogorov-Smirnov two sample test matrices demonstrating the similarity between (a–c) original size distributions and (d–e) logarithmic size distributions. Each square represents a comparison between a measurement site on the *x* axis and a measurement site on the *y* axis, where the color refers to the degree of similarity between the two distributions, dark blue being identical and yellow being less similar. The red line on the color bar highlights the critical value above which the distributions are not statistically similar for a significance level of 5%. The percentage of the comparisons that are statistically significant is quoted for each fan's matrices.

modern riverbed on each fan, we measure broad size distributions at the fan apices, with a D_{50} ranging between 74 and 135 mm. Downstream the size distributions fine and become narrower. We measured exponential rates of downstream fining of -0.019/km for the largest fan, ~ 40 km long, and ~ -0.068/km for two fans, ~ 25 km long. The standard deviation of the local size distributions is found to narrow downstream at an equivalent rate to the mean, indicating that the distributions are scale invariant. Statistical analysis of the degree of self-similarity between size distributions demonstrates that similarity is strong, though weaker when coarse tails in the distributions are significant. This degree of self-similarity allows us to effectively apply a constant, relative mobility function for the reconstruction of bedload mobility by size selective transport. Although the physical grain size distributions are notably different, the relative mobility of gravel sizes in the distributions has statistically similar profiles. We characterize a mobility profile for alluvial fan settings, where the mean grain size is ~60–70% more likely to be in the substrate than in transport. Although lateral inputs of sediment from fan surface reworking have a local influence on the fans' grain size fining trends, they do not appear to make a significant difference to the self-similarity of the grain size distributions as a whole.

Appendix A

Kolmogorov-Smirnov two-sample test matrices enable the statistical similarity between distributions (equation 7) to be visualized (Figure A1). Figure A1 demonstrates that a log transformation increases the similarity between distributions; most significantly on fans 2 and 3. The increase in similarity with the log transformation highlights the importance of the coarse tails of the distributions in causing a deviation from similarity

References

Allen, P. A. (2017). *Sediment routing systems: The fate of sediment from source to sink*. Cambridge: Cambridge University Press. https://doi.org/10.1017/9781316135754

Allen, P. A., Armitage, J. J., Carter, A., Duller, R. A., Michael, N. A., Sinclair, H. D., et al. (2013). The Qs problem: Sediment volumetric balance of proximal foreland basin systems. *Sedimentology*, *60*(1), 102–130. https://doi.org/10.1111/sed.12015

Allen, P. A., Michael, N. A., D'Arcy, M., Roda-Boluda, D. C., Whittaker, A. C., Duller, R. A., & et al. (2017). Fractionation of grain size in terrestrial sediment routing systems. *Basin Research*, *29*(2), 180–202. https://doi.org/10.1111/bre.12172

Andrews, E. D. (1984). Bed-material entrainment and hydraulic geometry of gravel-bed rivers in Colorado. *Geological Society of America Bulletin*, *95*(3), 371–378. https://doi.org/10.1130/0016-7606

Attal, M., & Lave, J. (2006). Changes of bedload characteristics along the Marsyandi River (central Nepal): Implications for understanding hillslope sediment supply, sediment load evolution along fluvial networks, and denudation in active orogenic belts. *Tectonics, Climate, and Landscape Evolution*, *398*, 143–171. https://doi.org/10.1130/2006.2398(09)

Attal, M., Mudd, S. M., Hurst, M. D., Weinman, B., Yoo, K., & Naylor, M. (2015). Impact of change in erosion rate and landscape steepness on hillslope and fluvial sediments grain size in the Feather River basin (Sierra Nevada, California). *Earth Surface Dynamics*, *3*(1), 201–222. https://doi.org/10.5194/esurf-3-201-2015

Bookhagen, B., & Strecker, M. R. (2012). Spatiotemporal trends in erosion rates across a pronounced rainfall gradient: Examples from the southern Central Andes. *Earth and Planetary Science Letters*, *327-328*, 97–110. https://doi.org/10.1016/j.epsl.2012.02.005

Buffington, J. M. (2012). Changes in channel morphology over human time scales. In M. Church, P. M. Biron, & A. G. Roy (Eds.), *Gravel-bed rivers: Processes, tools, environments*, (pp. 435–463). Chichester, UK: Wiley. https://doi.org/10.1002/9781119952497.ch32

Bunte, K., and S. R. Abt (2001), Sampling surface and subsurface particle-size distributions in wadable gravel-and cobble-bed streams for analysis in sediment transport, hydraulics and stream bed monitoring, Gen. Tech Rep. RMS-GTR-74*Rep.*, 428 pp, United States Department of Agriculture, Forest Service, Rocky Mountain Research Station, Fort Collins, CO.

Burke, K., Francis, P., & Wells, G. (1990). Importance of the geological record in understanding global change. *Global and Planetary Change*, *3*(3), 193–204. https://doi.org/10.1016/0921-8181(90)90016-6

Carretier, S., Regard, V., Vassallo, R., Aguilar, G., Martinod, J., Riquelme, R., et al. (2013). Slope and climate variability control of erosion in the Andes of central Chile. *Geology*, *41*(2), 195–198. https://doi.org/10.1130/G33735.1

Carretier, S., Tolorza, V., Rodríguez, M. P., Pepin, E., Aguilar, G., Regard, V., et al. (2015). Erosion in the Chilean Andes between 27°S and 39°S: tectonic, climatic and geomorphic control. *Geodynamic Processes in the Andes of Central Chile and Argentina*, *399*, 401–418. https://doi.org/10.1144/Sp399.16

Coulthard, T. J., Lewin, J., & Macklin, M. G. (2005). Modelling differential catchment response to environmental change. *Geomorphology*, *69*(1–4), 222–241. https://doi.org/10.1016/j.geomorph.2005.01.008

Cui, Y. T., Parker, G., & Paola, C. (1996). Numerical simulation of aggradation and downstream fining. *Journal of Hydraulic Research*, *34*(2), 185–204. https://doi.org/10.1080/00221689609498496

D'Arcy, M., Whittaker, A. C., & Roda-Boluda, D. C. (2017). Measuring alluvial fan sensitivity to past climate changes using a self-similarity approach to grain-size fining, Death Valley, California. *Sedimentology*, *64*(2), 388–424. https://doi.org/10.1111/sed.12308

Densmore, A. L., Allen, P. A., & Simpson, G. (2007). Development and response of a coupled catchment fan system under changing tectonic and climatic forcing. *Journal of Geophysical Research*, *112*, F01002. https://doi.org/10.1029/2006jf000474

Dietrich, W. E., Kirchner, J. W., Ikeda, H., & Iseya, F. (1989). Sediment supply and the development of the coarse surface-layer in gravel-bedded rivers. *Nature*, *340*(6230), 215–217. https://doi.org/10.1038/340215a0

Duller, R. A., Whittaker, A. C., Fedele, J. J., Whitchurch, A. L., Springett, J., Smithells, R., et al. (2010). From grain size to tectonics. *Journal of Geophysical Research*, *115*, F03022. https://doi.org/10.1029/2009jf001495

Fedele, J. J., & Paola, C. (2007). Similarity solutions for fluvial sediment fining by selective deposition. *Journal of Geophysical Research*, *112*, F02038. https://doi.org/10.1029/2005jf000409

Ferguson, R., Hoey, T., Wathen, S., & Werritty, A. (1996). Field evidence for rapid downstream fining of river gravels through selective transport. *Geology*, *24*(2), 179–182. https://doi.org/10.1130/0091-7613

Ferguson, R. I., Cudden, J. R., Hoey, T. B., & Rice, S. P. (2006). River system discontinuities due to lateral inputs generic styles and controls. *Earth Surface Processes and Landforms*, *31*(9), 1149–1166. https://doi.org/10.1002/esp.1309

Ferguson, R. I., & Paola, C. (1997). Bias and precision of percentiles of bulk grain size distributions. *Earth Surface Processes and Landforms*, *22*(11), 1061–1077. https://doi.org/10.1002/(Sici)1096-9837

Forte, A. P., Villarroel, C. D., & Esper Angillieri, M. Y. (2016). Impact of natural parameters on rock glacier development and conservation in subtropical mountain ranges. Northern sector of the Argentine Central Andes. *The Cryosphere Discussions*, 1–24. https://doi.org/10.5194/tc-2016-232

Forzoni, A., Storms, J. E. A., Whittaker, A. C., & de Jager, G. (2014). Delayed delivery from the sediment factory: Modeling the impact of catchment response time to tectonics on sediment flux and fluvio-deltaic stratigraphy. *Earth Surface Processes and Landforms*, *39*(5), 689–704. https://doi.org/10.1002/esp.3538

Giambiagi, L., Mescua, J., Bechis, F., Tassara, A., & Hoke, G. (2012). Thrust belts of the southern Central Andes: Along-strike variations in shortening, topography, crustal geometry, and denudation. *Geological Society of America Bulletin*, *124*(7–8), 1339–1351. https://doi.org/10.1130/B30609.1

Goodbred, S. L. (2003). Response of the Ganges dispersal system to climate change: A source-to-sink view since the last interstade. *Sedimentary Geology*, *162*(1–2), 83–104. https://doi.org/10.1016/S0037-0738(03)00217-3

Guerit, L., Metivier, F., Devauchelle, O., Lajeunesse, E., & Barrier, L. (2014). Laboratory alluvial fans in one dimension. *Physical Review E*, *90*(2). https://doi.org/10.1103/PhysRevE.90.022203

Hales, T. C., & Roering, J. J. (2007). Climatic controls on frost cracking and implications for the evolution of bedrock landscapes. *Journal of Geophysical Research*, *112*, F02033. https://doi.org/10.1029/2006jf000616

Haschenburger, J. K., & Wilcock, P. R. (2003). Partial transport in a natural gravel bed channel. *Water Resources Research*, *39*(1), 1020. https://doi.org/10.1029/2002wr001532

Hijmans, R. J., Cameron, S. E., Parra, J. L., Jones, P. G., & Jarvis, A. (2005). Very high resolution interpolated climate surfaces for global land areas. *International Journal of Climatology*, *25*(15), 1965–1978. https://doi.org/10.1002/joc.1276

Hirano, M. (1971). River bed degradation with armouring. *Proceedings of the Japanese Society of Civil Engineering*, *195*, 55–65.

Hoey, T. B., & Bluck, B. J. (1999). Identifying the controls over downstream fining of river gravels. *Journal of Sedimentary Research*, *69*(1), 40–50. https://doi.org/10.2110/jsr.69.40

Hoke, G. D., Giambiagi, L. B., Garzione, C. N., Mahoney, J. B., & Strecker, M. R. (2014). Neogene paleoelevation of intermontane basins in a narrow, compressional mountain range, southern Central Andes of Argentina. *Earth and Planetary Science Letters*, *406*, 153–164. https://doi.org/10.1016/j.epsl.2014.08.032

Hooke, R. L., & Rohrer, W. L. (1979). Geometry of alluvial fans - effect of discharge and sediment size. *Earth Surface Processes and Landforms*, *4*(2), 147–166. https://doi.org/10.1002/esp.3290040205

Le Houérou, H. N., Martinez-Carretero, E., Guevara, J. C., Berra, A. B., Estevez, O. R., & Stasi, C. R. (2006). The true desert of the central-west Argentina: Bioclimatology, Geomorphology and vegetation. *Multequina*, *15*, 1–15.

Humphrey, N. F., & Heller, P. L. (1995). Natural oscillations in coupled geomorphic systems - an alternative origin for cyclic sedimentation. *Geology*, *23*(6), 499–502. https://doi.org/10.1130/0091-7613

Jerolmack, D. J., & Paola, C. (2010). Shredding of environmental signals by sediment transport. *Geophysical Research Letters*, *37*, L19401. https://doi.org/10.1029/2010gl044638

Jones, R. E., De Hoog, J. C. M., Kirstein, L. A., Kasemann, S. A., Hinton, R., Elliott, T., et al., & EIMF (2014). Temporal variations in the influence of the subducting slab on central Andean arc magmas: Evidence from boron isotope systematics. *Earth and Planetary Science Letters*, *408*, 390–401. https://doi.org/10.1016/j.epsl.2014.10.004

Jordan, T. E., Allmendinger, R. W., Damanti, J. F., & Drake, R. E. (1993). Chronology of motion in a complete thrust belt - the precordillera, 30–31°S, Andes mountains. *Journal of Geology*, *101*(2), 135–156. https://doi.org/10.1086/648213

Kellerhals, R., & Bray, D. I. (1971). Sampling procedures for coarse fluvial sediments. Journal of the Hydraulics Division. *American Society of Civil Engineers*, *97*, 1165–1180.

Kim, W., Petter, A., Straub, K., & Mohrig, D. (2014). Investigating the autogenic process response to allogenic forcing: Experimental geomorphology and stratigraphy. *International Journal of Sediment*, *46*, 127–138.

Laronne, J. B., Reid, I., Yitshak, Y., & Frostick, L. E. (1994). The non-layering of gravel streambeds under ephemeral flood regimes. *Journal of Hydrology*, *159*(1–4), 353–363. https://doi.org/10.1016/0022-1694(94)90266-6

Legarreta, L., Uliana, M. A., Larotonda, C. A., & Meconi, G. R. (1993), Approaches to nonmarine sequence stratigraphy-theoretical models and examples from Argentine basins, In: Eschard, R. and Doligez, B., (eds.), Subsurface Reservoir Characterization from Outcrop Observation, Proceedings of the 7th Exploration and production Research Conference, Institute Francais du Petrole, Editions Technip, Paris, 51, 125-143.

Malatesta, L. C., Prancevic, J. P., & Avouac, J.-P. (2017). Autogenic entrenchment patterns and terraces due to coupling with lateral erosion in incising alluvial channels. *Journal Of Geophysical Research: Earth Surface*, *122*, 335–355. https://doi.org/10.1002/2015JF003797

Millar, R. G. (2005). Theoretical regime equations for mobile gravel-bed rivers with stable banks. *Geomorphology*, *64*(3–4), 207–220. https://doi.org/10.1016/j.geomorph.2004.07.001

Miller, K. L., Reitz, M. D., & Jerolmack, D. J. (2014). Generalized sorting profile of alluvial fans. *Geophysical Research Letters*, *41*, 7191–7199. https://doi.org/10.1002/2014gl060991

Minetti, J., Barbieri, P., Carletto, M., Poblete, A., & Sierra, E. (1986). El régimen de precipitaciones de San Juan y su entorno, centro de investigaciones regionales de San Juan (CIRSAJ). *Informe Técnico*, *8*, 19–22.

Molnar, P., & England, P. (1990). Late Cenozoic uplift of mountain-ranges and global climate change - chicken or egg. *Nature*, *346*(6279), 29–34. https://doi.org/10.1038/346029a0

Mueller, E. R., Pitlick, J., & Nelson, J. M. (2005). Variation in the reference Shields stress for bed load transport in gravel-bed streams and rivers. *Water Resources Research*, *41*, W04006. https://doi.org/10.1029/2004wr003692

Nicholas, A. P., & Quine, T. A. (2007). Modeling alluvial landform change in the absence of external environmental forcing. *Geology*, *35*(6), 527–530. https://doi.org/10.1130/G23377a.1

Paola, C., Heller, P. L., & Angevine, C. L. (1992). The large-scale dynamics of grain-size variation in alluvial basins, 1 Theory. *Basin Research*, *4*(2), 73–90. https://doi.org/10.1111/j.1365-2117.1992.tb00145.x

Paola, C., Parker, G., Seal, R., Sinha, S. K., Southard, J. B., & Wilcock, P. R. (1992). Downstream fining by selective deposition in a laboratory flume. *Science*, *258*(5089), 1757–1760. https://doi.org/10.1126/science.258.5089.1757

Paola, C., & Seal, R. (1995). Grain-size patchiness as a cause of selective deposition and downstream fining. *Water Resources Research*, *31*, 1395–1407. https://doi.org/10.1029/94wr02975

Paola, C., & Voller, V. R. (2005). A generalized Exner equation for sediment mass balance. *Journal of Geophysical Research*, *110*, F04014. https://doi.org/10.1029/2004jf000274

Parker, G. (1978). Self-formed straight rivers with equilibrium banks and mobile bed.2. Gravel river. *Journal of Fluid Mechanics*, *89*(01), 127. https://doi.org/10.1017/S0022112078002505

Parker, G. (1991). Selective sorting and abrasion of river gravel.2. Applications. *Journal of Hydraulic Engineering*, *117*(2), 150–171. https://doi.org/10.1061/(Asce)0733-9429(1991)117:2(150)

Parker, G., & Toro-Escobar, C. M. (2002). Equal mobility of gravel in streams: The remains of the day. *Water Resources Research*, *38*(11), 1264. https://doi.org/10.1029/2001WR000669

Parker, G., Wilcock, P. R., Paola, C., Dietrich, W. E., & Pitlick, J. (2007). Physical basis for quasi-universal relations describing bankfull hydraulic geometry of single-thread gravel bed rivers. *Journal of Geophysical Research*, *112*, F04005. https://doi.org/10.1029/2006jf000549

Parsons, A. J., Michael, N. A., Whittaker, A. C., Duller, R. A., & Allen, P. A. (2012). Grain-size trends reveal the late orogenic tectonic and erosional history of the south-central Pyrenees, Spain. *Journal of the Geological Society of London*, *169*(2), 111–114. https://doi.org/10.1144/0016-76492011-087

Penna, I., Hermanns, R. L., Juboyedoff, M., & Fauque, L. (2016). Large scale rockslides in the Argentine Andes: Distribution and forcing factors. In *Landslides and Engineered Slopes. Experience, Theory and Practice*, (pp. 1599–1603). Rome, Italy: Associazione Geotecnica Italiana. https://doi.org/10.1201/b21520-198

Perucca, L. P., & Martos, L. M. (2012). Geomorphology, tectonism and Quaternary landscape evolution of the central Andes of San Juan (30°S–69°W), Argentina. *Quaternary International*, *253*, 80–90. https://doi.org/10.1016/j.quaint.2011.08.009

Polanski, J. (1963). Estratigrafia, neotectonica y geomorfologia del Pleistoceno pedemontano, entre los rios Diamante y Mendoza. *Revista de la Asociación Geológica Argentina*, *17*(3–4), 127–349.

Powell, D. M. (1998). Patterns and processes of sediment sorting in gravel-bed rivers. *Progress in Physical Geography*, *22*(1), 1–32. https://doi.org/10.1177/030913339802200101

Pratt-Sitaula, B., Garde, M., Burbank, D. W., Oskin, M., Heimsath, A., & Gabet, E. (2007). Bedload-to-suspended load ratio and rapid bedrock incision from Himalayan landslide-dam lake record. *Quaternary Research*, *68*(01), 111–120. https://doi.org/10.1016/j.yqres.2007.03.005

Rice, S. (1999). The nature and controls on downstream fining within sedimentary links. *Journal of Sedimentary Research*, *69*(1), 32–39. https://doi.org/10.2110/jsr.69.32

Rice, S., & Church, M. (1996). Sampling surficial fluvial gravels: The precision of size distribution percentile estimates. *Journal of Sedimentary Research*, *66*(3), 654–665. https://doi.org/10.2110/jsr.66.654

Rice, S., & Church, M. (1998). Grain size along two gravel-bed rivers: Statistical variation, spatial pattern and sedimentary links. *Earth Surface Processes and Landforms*, *23*(4), 345–363. https://doi.org/10.1002/(Sici)1096-9837(199804)23:4

Roda-Boluda, D. C., D'Arcy, M., McDonald, J., & Whittaker, A. C. (2018). Lithological controls on hillslope sediment supply: Insights from landslide activity and grain size distributions. *Earth Surface Processes and Landforms*, *43*(5), 956–977. https://doi.org/10.1002/esp.4281

Savi, S., Schildgen, T. F., Tofelde, S., Wittmann, H., Scherler, D., Mey, J., et al. (2016). Climatic controls on debris-flow activity and sediment aggradation: The Del Medio fan, NW Argentina. *Journal of Geophysical Research: Earth Surface*, *121*, 2424–2445. https://doi.org/10.1002/2016jf003912

Schumm, S. A. (1979). Geomorphic thresholds - concept and its applications. *Transactions of the Institute of British Geographers*, *4*(4), 485–515. https://doi.org/10.2307/622211

Seal, R., & Paola, C. (1995). Observations of downstream fining on the North Fork Toutle River near Mount St-Helens, Washington. *Water Resources Research*, *31*, 1409–1419. https://doi.org/10.1029/94wr02976

Seal, R., Paola, C., Parker, G., Southard, J. B., & Wilcock, P. R. (1997). Experiments on downstream fining of gravel.1. Narrow-channel runs. *Journal of Hydraulic Engineering-Asce*, *123*(10), 874–884. https://doi.org/10.1061/(Asce)0733-9429(1997)123:10(874)

Sepulveda, S. A., Giambiagi, L. B., Moreiras, S. M., Pinto, L., Tunik, M., Hoke, G. D., & et al. (2015). Geodynamic processes in the Andes of Central Chile and Argentina: An introduction. *Geodynamic Processes in the Andes of Central Chile and Argentina*, *399*(1), 1–12. https://doi.org/10.1144/Sp399.21

Shields, A. (1936), Awendung der aehnlichkeitsmechanik und der turbulenzforschung auf die geschiebebewegung, Mltt. Preuss. Versuchsanst. Wasserbau Schiffau, 26.

Siame, L. L., Bourles, D. L., Sebrier, M., Bellier, O., Castano, J. C., Araujo, M., et al. (1997). Cosmogenic dating ranging from 20 to 700 ka of a series of alluvial fan surfaces affected by the El Tigre fault, Argentina. *Geology*, *25*(11), 975–978. https://doi.org/10.1130/0091-7613(1997)025

Sklar, L. S., Fadde, J., Venditti, J. G., Nelson, P., Wydzga, M. A., Cui, Y. T., & et al. (2009). Translation and dispersion of sediment pulses in flume experiments simulating gravel augmentation below dams. *Water Resources Research*, *45*, W08439. https://doi.org/10.1029/2008wr007346

Sternberg, H. (1875). Untersuchungen über langen-und querprofil geschiebeführende flüsse. *Zeitschrift für Bauwesen*, *25*, 483–506.

Straub, K. M., & Esposito, C. R. (2013). Influence of water and sediment supply on the stratigraphic record of alluvial fans and deltas: Process controls on stratigraphic completeness. *Journal of Geophysical Research: Earth Surface*, *118*, 625–637. https://doi.org/10.1002/jgrf.20061

Straub, K. M., & Wang, Y. A. (2013). Influence of water and sediment supply on the long-term evolution of alluvial fans and deltas: Statistical characterization of basin-filling sedimentation patterns. *Journal of Geophysical Research: Earth Surface*, *118*, 1602–1616. https://doi.org/10.1002/jgrf.20095

Syvitski, J. P. M., & Milliman, J. D. (2007). Geology, geography, and humans battle for dominance over the delivery of fluvial sediment to the coastal ocean. *Journal of Geology*, *115*(1), 1–19. https://doi.org/10.1086/509246

Toro-Escobar, C. M., Parker, G., & Paola, C. (1996). Transfer function for the deposition of poorly sorted gravel in response to streambed aggradation. *Journal of Hydraulic Research*, *34*(1), 35–53. https://doi.org/10.1080/00221689609498763

Turowski, J. M., Rickenmann, D., & Dadson, S. J. (2010). The partitioning of the total sediment load of a river into suspended load and bedload a review of empirical data, Sedimentology Volume 57, Issue 4. *Sedimentology*, *57*(4), 1126–1146. https://doi.org/10.1111/j.1365-3091.2009.01140.x

Van De Wiel, M. J., & Coulthard, T. J. (2010). Self-organized criticality in river basins: Challenging sedimentary records of environmental change. *Geology*, *38*(1), 87–90. https://doi.org/10.1130/G30490.1

Venditti, J. G., Dietrich, W. E., Nelson, P. A., Wydzga, M. A., Fadde, J., & Sklar, L. (2010a). Effect of sediment pulse grain size on sediment transport rates and bed mobility in gravel bed rivers. *Journal of Geophysical Research*, *115*, F03039. https://doi.org/10.1029/2009jf001418

Venditti, J. G., Dietrich, W. E., Nelson, P. A., Wydzga, M. A., Fadde, J., & Sklar, L. (2010b). Mobilization of coarse surface layers in gravel-bedded rivers by finer gravel bed load. *Water Resources Research*, *46*, W07506. https://doi.org/10.1029/2009wr008329

Voldoire, A., Sanchez-Gomez, E., Salas y Mélia, D., Decharme, B., Cassou, C., Sénési, S., et al. (2013). The CNRM-CM5.1 global climate model: Description and basic evaluation. *Climate Dynamics*, *40*(9–10), 2091–2121. https://doi.org/10.1007/s00382-011-1259-y

Whittaker, A. C., Duller, R. A., Springett, J., Smithells, R. A., Whitchurch, A. L., & Allen, P. A. (2011). Decoding downstream trends in stratigraphic grain size as a function of tectonic subsidence and sediment supply. *Geological Society of America Bulletin*, *123*(7–8), 1363–1382. https://doi.org/10.1130/B30351.1

Wilcock, P. R., & McArdell, B. W. (1993). Surface-based fractional transport rates mobilization thresholds and partial transport of a sand-gravel sediment, Water Resources Research Volume 29, Issue 4. *Water Resources Research*, *29*, 1297–1312. https://doi.org/10.1029/92WR02748

Wilcock, P. R., & McArdell, B. W. (1997). Partial transport of a sand/gravel sediment. *Water Resources Research*, *33*, 235–245. https://doi.org/10.1029/96WR02672

Wilcock, P. R., & Southard, J. B. (1989). Bed load transport of mixed size sediment fractional transport rates, bed forms, and the development of a coarse bed surface layer. *Water Resources Research*, *25*, 1629–1641. https://doi.org/10.1029/WR025i007p01629

Zarate, M. A., & Mehl, A. E. (2008). Estratigrafia y geocronologia de los depositos del Pleistoceno tardio/Holoceno de la cuenca del arroyo La Estacada, departamentos de Tunuyan y Tupungato (Valle de Uco), Mendoza. *Revista de la Asociación Geológica Argentina*, *63*(3), 407–416.